J. Fluid Mech. (1990), *vol.* 218, *pp.* 71–107
Printed in Great Britain

On the formation and suppression of vortex 'shedding' at low Reynolds numbers

By P. J. STRYKOWSKI[1] AND K. R. SREENIVASAN[2]

[1]Department of Mechanical Engineering, University of Minnesota, Minneapolis, MN 55455, USA
[2]Mason Laboratory, Yale University, New Haven, CT 06520, USA

(Received 9 January 1989 and in revised form 6 December 1989)

Vortex 'shedding' behind circular cylinders can be altered and suppressed altogether (or 'controlled') over a limited range of Reynolds numbers, by a proper placement of a second, much smaller, cylinder in the near wake of the main cylinder. This new and dramatic suppression of vortex 'shedding' is the subject of this paper. Details of the phenomenon are documented through parallel experimental and numerical investigations, including flow visualization. Temporal growth rate measurements of the velocity fluctuations reveal that the presence of the smaller cylinder reduces the growth rate of the disturbances leading to vortex 'shedding', and that its suppression, accompanied by the disappearance of sharp spectral peaks, coincides with negative temporal growth rates. It is argued that the presence of the secondary cylinder has the effect of altering the local stability of the flow by smearing and diffusing concentrated vorticity in the shear layers behind the body; a related effect is that the secondary cylinder diverts a small amount of fluid into the wake of the main cylinder. A unified explanation of the formation and suppression of the vortex street is attempted, and it is suggested that the vortex 'shedding' is associated with temporally unstable eigenmodes which are heavily weighted by the near field. It is also shown that absolute instability is relevant, up to a point, in explaining vortex shedding, whose suppression can similarly be associated with altering the instability in the near wake region from absolute to convective.

1. Introduction

The phenomenon of vortex 'shedding'† behind bluff bodies is familiar since the days of Leonardo da Vinci, and has been studied systematically at least since the days of Strouhal (1878). Many important contributions have been made, and a partial list includes Kármán (1911), Kármán & Rubach (1912), Fage & Johansen (1927, 1928), Kovasznay (1949), Roshko (1954), Tritton (1959), Abernathy & Kronaur (1961), Berger (1964) and Gerrard (1966). Much information has been accumulated, but it is fair to say that the present understanding is far from complete.

The basic observation on which we elaborate in this paper is the ease with which the nature of vortex shedding behind bluff bodies can be altered, at least at low Reynolds numbers. We report results from experiments primarily (but not exclusively) on flow behind circular cylinders, and emphasize a novel method of suppression of low-Reynolds-number vortex shedding. The experimental findings are substantiated by full-scale numerical simulation. We present these results not only

† No specific physical process is implied by the use of the word 'shedding' which, for convenience, will be used subsequently without the quotes.

because of their novelty but also because they add, as we hope to demonstrate, to our understanding of the physical processes associated with the occurrence of vortex shedding behind bluff bodies.

The sensitivity of vortex shedding at low Reynolds numbers to small external perturbations has long been known. Kovasznay (1949) indicated that a hot-wire probe positioned with supports aligned parallel to the flow caused an upstream-propagating instability. Mair & Maull (1971) reported Berger's remarks that the vortex shedding frequency over the entire span of the cylinder dropped when a hot wire was inserted in one of the shear layers, and that this effect depended on the overheat ratio of the hot wire. Berger has added in private conversation with us that this frequency, measured in one of the shear layers approximately 20 diameters downstream of the cylinder (0.5 mm diameter), was reduced (merely because of hot-wire insertion) by about 30%. The Reynolds number Re, based on the oncoming free-stream velocity U_0 and the cylinder diameter D, was about 90.

Cylinder vibrations and other streaming techniques are known to produce many interesting effects characteristic of a nonlinear self-excited oscillator (for a survey, see Mair & Maull 1971; Berger & Wille 1972; for a new perspective relating to the so-called 'universal' behaviour in this nonlinear system, see Olinger & Sreenivasan 1988*a*, *b*). Among these effects, special mention must be made of vortex suppression. Berger (1967) showed that the vortex shedding in the wake of a cylinder with an oval cross-section could be suppressed in a narrow Reynolds-number range ($77 < Re < 80$, Re here based on the cylinder width) by vibrating the cylinder at frequencies several times the vortex shedding frequency. Wehrmann (1967), also working with oval cylinders, noted a similar effect at Reynolds numbers between 40 and 80.

Geometrical modifications further illustrating the sensitivity of the vortex shedding process include the influence of end plates (Stansby 1974; Nishioka & Sato 1974), flow non-uniformities (Gaster 1969, 1971; Gerich & Eckelmann 1982), use of splitter plates (Roshko 1955), base bleed (Bearman 1967), blockage effects (Shair *et al.* 1963), etc.

At present, the reasons for this wake sensitivity are not fully understood. We intend to show that this is a manifestation of the fact that *global* changes in the wake can be produced through only *local* modifications. After a brief description in §2 of experimental facilities, we outline this basic feature in §3 by showing that vortex formation at low Reynolds numbers can be completely suppressed by suitably placing in the wake of the vortex shedding cylinder a much smaller cylinder, to be called here the 'control' or secondary cylinder. These findings are substantiated in §4 by the numerical investigation of the wake with and without the secondary cylinder by solving the incompressible Navier–Stokes equations using a two-dimensional finite-difference Galerkin method. In §5, we briefly describe related suppression observations on other bluff bodies, and the effect of heating the control cylinder. We elucidate in §6 the suppression phenomenon by concentrating on the temporally unstable modes and their relevance to vortex shedding; further insight is obtained from power spectral measurements. Finally, in §7, these observations are interpreted in terms of the alteration of the nature of instability that the secondary cylinder produces; we especially discuss whether these features can be explained by the notion that the near wake of bluff bodies is governed by an absolute instability (Koch 1985; Huerre & Monkewitz 1985; Triantafyllou, Triantafyllou & Chryssostomidis 1986; Monkewitz & Nguyen 1987; Monkewitz 1988; Hannemann & Oertel 1989).

A preliminary and partial account of the experimental aspects of this work appeared in Strykowski & Sreenivasan (1985*a*).

2. Experimental facilities and instrumentation

2.1. *Wind tunnels*

Measurements were made in pressure-driven wind tunnels, supplied with compressed dry air from two large storage tanks (combined storage volume of approximately 18 m^3 at a storage pressure of 8×10^5 N/m^2), thus eliminating sizeable discrete frequencies usually associated with blowers. One of the tunnels was a carefully designed, low-turbulence facility. The second tunnel was designed especially for measuring temporal growth and decay rates in the wake. A brief description of the facilities is provided below.

2.1.1. *Low-turbulence facility*

Air entered two settling chambers packed with damping material, downstream of which were two tandem contractions with several carefully placed screens in between; see Strykowski (1986) for details. The settling chambers were acoustically lined with convoluted foam, and the upstream and downstream contractions had area ratios of 9:1 and 6:1 respectively. The whole arrangement produced, with the test-section empty, a turbulence level $u'/U_0 < 0.03\%$ over the range of velocities investigated; u' here is the root-mean-square (r.m.s.) magnitude of the streamwise velocity whose mean is U_0. The r.m.s. turbulence levels were measured from hot-wire signals filtered from DC to 5 kHz and integrated over long time intervals (typically a minute). Downstream of the second contraction was a test chamber of circular cross-section. The test section was 5 cm in diameter and 10 cm long; its area was carefully diverged to produce constant velocity throughout. The flow velocity entering the test section downstream of the second contraction was uniform across the test section (outside the boundary layers) to within 1%.

2.1.2. *Tunnel designed to measure amplification and decay rates*

A second wind tunnel was employed to measure the temporal growth and decay rates of wake oscillations (to be discussed in §6). The tunnel provided a steady mean flow but was designed with only a single contraction and could not be considered a 'low turbulence' facility ($u'/U_0 \sim 0.15\%$). Upstream of the settling chamber were placed large needle and globe valves. The needle valve was used to adjust the speed, and the globe valve enabled the air flow to be rapidly established or quenched; this ability is critical for the transient experiments to be described in §6. To enhance the response of the system, relatively large pipes were used to connect the settling chamber to the two storage tanks.

2.2. *Flow quality*

Before detailed measurements were made, both wind tunnels were checked for flow non-uniformities which might result in a 'cell' structure as described by Gaster (1971) and Gerich & Eckelmann (1982). The low-turbulence-level tunnel produced, in the Reynolds-number range of 40 to 100, no cell structure over most of the cylinder. The single-contraction wind tunnel contained three cells due to small mean flow irregularities. The cells were approximately stationary at the flow speeds of

Facility	D (cm)	D/d	L/D	H/D
Water channel	0.32	7	15	80
Low-turbulence wind tunnel	0.08	3	60	60
	0.08	7.5	60	60
	0.08	10.0	60	60
	0.08	15.0	60	60
	0.08	20.0	60	60
Single-contraction wind tunnel	0.15	10.0	60	72
	0.15	10.0	27	72
	0.15	10.0	14	72
	0.32	10.0	60	33

TABLE 1. Data on the cylinders and flow facilities used in the experiments: D, the diameter of the main or vortex shedding cylinder; d, control cylinder diameter; L, cylinder length between end plates, the span; H, height of the test section normal to the cylinder axis and the free stream

interest, and therefore a 'clean' slice of the flow was selected with properly placed end plates designed after Stansby (1974).

Well polished drill rods were used as cylinders and were fitted with end plates to provide better end conditions. Owing to the relatively small dimensions of the cylinders, the end plates were anchored to the tunnel sidewalls and the cylinders passed through narrow openings machined into the end plates. The relevant data concerning the cylinders and flow facilities are presented in table 1, which also includes the dimensions of the secondary or 'control' cylinder discussed below.

2.3. *Instrumentation*

Some of the results to follow were obtained with DANTEC constant-temperature hot-wire anemometers, type 55M01, using 5 μm wires etched to a working length of approximately 0.8 mm; overheat ratios of 1.75 were used. The resulting data were DC offset and filtered with a DANTEC signal conditioner, model 55D26, and amplified to optimize the 12-bit resolution (± 5 V) of the MASSCOMP MC-5000 series computer. All data processing was done on this machine. During the initial stages of the work, it was felt that the hot-wire probe, when placed within a few diameters of the cylinder, might be intruding on some details of flow development (see Kovasznay 1949; Mair & Maull 1971; and below). Thus, all hot-wire measurements were made outside of this sensitive region. Within this region, velocity measurements were made with a TSI laser Doppler velocimeter (LDV) in the forward scatter mode. In instances where both LDV and hot wire were deemed reliable, both were used under identical circumstances as a check on each other.

The power spectral data were Bartlett averaged over four record lengths of 16000 points each providing a spectral resolution of $\Delta f = 0.24$ Hz (compared with the vortex shedding frequency typically in the range of 200 Hz). Discrete peaks in the power spectra found below about 50 Hz have been investigated, and a detailed account of their source as well as their minor effects can be found in Strykowski (1986). It suffices here to say that they are of minor magnitude (see §6.4), and do not affect the development of the wake in any significant way. It is important to stress that the following observations were independent of which flow facility was used, and that the essential aspects have in fact been repeated in several laboratories elsewhere since the first observations made by us.

Flow visualization was performed in a water channel (Technovate model 9045) with a free surface; the working depth of water was approximately 5 cm. Hydrogen bubbles generated from 0.05 mm steel wires, tensioned across the test section orthogonal to the cylinder, were used as flow markers. Short time exposure photographs of the flow field were taken with a Minolta SRT202 camera fitted with a macro lens and a Vivitar 283 flash.

Mean velocity was obtained using a Pitot tube and an MKS-Baratron model 270B with a 10 Torr differential pressure head.

3. The basic experimental observations

3.1. *The phenomenon*

A hydrogen-bubble visualization of the vortex shedding behind a circular cylinder is shown in figure 1; the flow Reynolds number is about 80. In the facility employed for flow visualization, the natural vortex shedding did not commence until a Reynolds number of about 60, this being higher than the usual value of about 46 (see Nishioka & Sato 1974; Mathis, Provansal & Boyer 1984; and Strykowski 1986) because the aspect ratio L/D (L being the spanwise length of the cylinder) was low (about 15).

Let us now introduce another more slender cylinder (hereafter called the secondary or 'control' cylinder) of diameter d behind and parallel to the main cylinder (see figure 2), roughly in one of the shear layers. For a Reynolds number of about 80 and the control cylinder diameter $d = \frac{1}{7}D$, flow visualization clearly reveals that the vortex street is completely suppressed (figure 3). (It is worth emphasizing that the velocity fluctuations in the natural vortex street decay exponentially beyond a certain initial distance, and that the street survives only for finite distances which depends on the Reynolds number (Cimbala, Nagib & Roshko 1988).) Confirmation of this suppression is given in figure 4 by hot-wire time traces of the streamwise velocity recorded in a wind-tunnel flow under somewhat similar conditions (but the aspect ratio was about 60, and d/D was about half as small). All hot-wire measurements were made in the shear layer not occupied by the control cylinder. (Both figures 3 and 4 correspond to the so-called 'optimal position' to be described in §6.3 where a more general measure of suppression will be provided.)

When making hot-wire measurements, the control cylinder was carefully adjusted to be parallel to the main vortex shedding cylinder and was mounted on a micrometer base enabling accurate two-dimensional positioning. The control cylinder was tensioned and passed through holes in the end plates or the tunnel walls so that all supporting structure was removed from the flow field. Under no circumstances did the control cylinder produce its own vortex shedding. The control cylinder Reynolds number $U_0\, d/\nu$ was less than 10 in all those cases in which quantitative data were obtained, and never more than 25.

There is a finite spatial domain within which the placement of the control cylinder can suppress the vortex street. Figure 5 shows the regions of vortex suppression for four values of the diameter ratio D/d; clearly the region shrinks with increasing D/d. (A discussion of how the boundaries of these regions were defined precisely is best relegated to a subsequent section, but it suffices here to say that the boundaries are defined sharply enough that almost any definition will yield essentially the same results.) When the control cylinder is placed anywhere within these contours the vortex street is suppressed as completely as indicated in figures 3 and 4. Furthermore, the contours are symmetric about the line $y = 0$, indicating that a single control

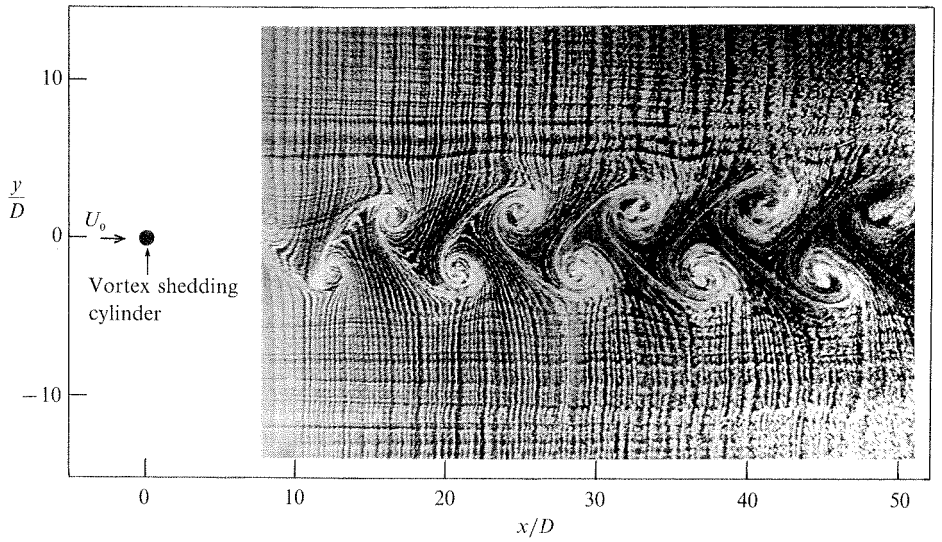

FIGURE 1. Hydrogen-bubble picture of vortex shedding behind a circular cylinder at $Re = 80$.

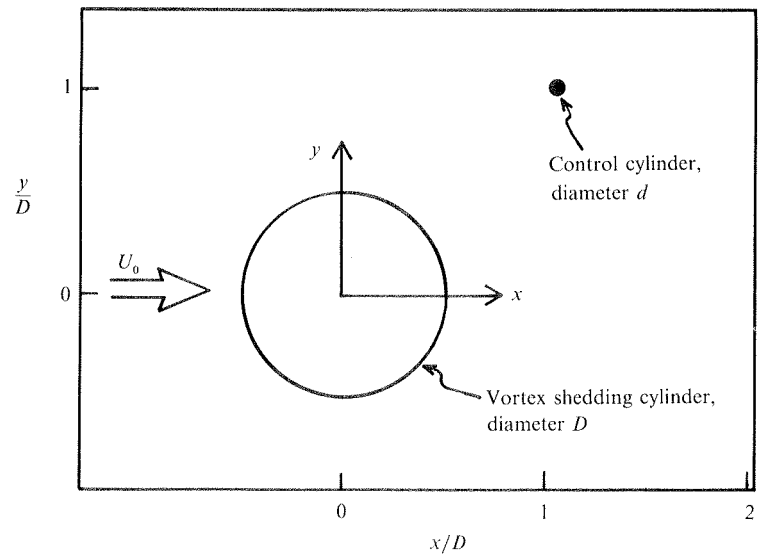

FIGURE 2. Schematic of the arrangement for control of vortex shedding; $D/d < 20$.

cylinder place on either side of the wake can be effective. At $Re = 80$, the largest value of the diameter ratio which was capable of vortex suppression was $D/d = 20$ for conditions in figure 5; in this case the region of control shrinks essentially to a point.

We should remark that the control cylinder effects are negligible except when it is positioned in the near-wake region (not farther than approximately 3.5 to 4 diameters downstream of the vortex shedding cylinder). The subtle changes produced near the main cylinder in this region can be seen qualitatively by a comparison of figure 6 (which is the natural vortex shedding case) with figures 7 and 8 corresponding to complete suppression; the Reynolds number in all these figures is

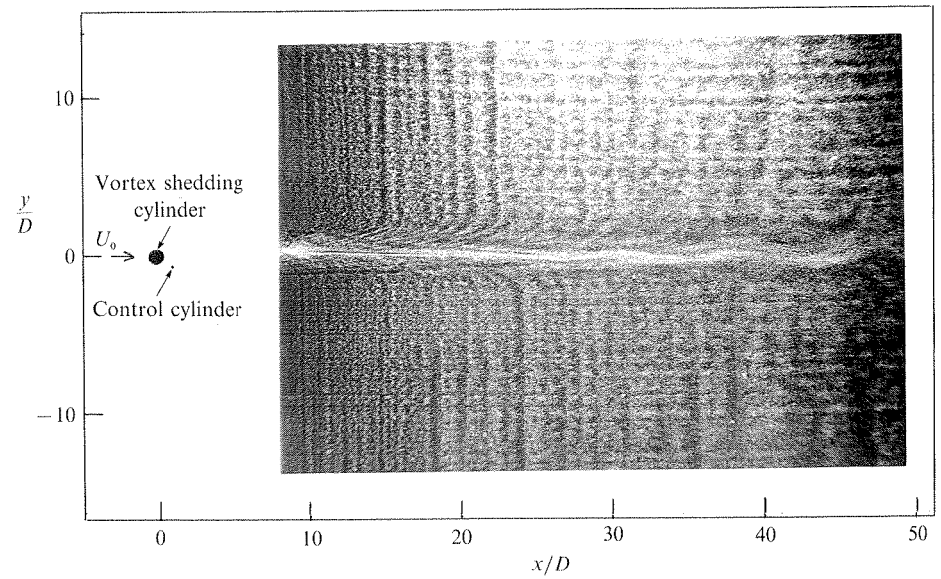

FIGURE 3. Hydrogen-bubble picture showing the control of vortex shedding at $Re = 80$ using a control cylinder of $D/d = 7$.

about 90 and $D/d = 7$. Note that the control cylinder in each of the figures 7 and 8 has the effect of diverting part of the fluid into the wake from outside, but the detailed conditions (such as the position of the control cylinder) are different between the two.

We have seen that the proper placement of a control cylinder suppresses vortex street formation at low Reynolds numbers up to about 80, the precise number depending on various conditions (these conditions are discussed in greater detail in §3.2). Now keeping the control cylinder in position, if the Reynolds number is further increased, the vortex street reappears at a higher Reynolds number. As we shall discuss later, the effect of the control cylinder is not merely to elevate the critical Reynolds number to a higher value, because the control cylinder produces a non-trivial influence even at Reynolds numbers above which complete suppression is impossible. These changes are demonstrated qualitatively in the following experiment. We introduce the control cylinder at $x/D = 1.2$ but well removed from the wake, say $y/D > 20$, and gradually move it closer to the main shedding cylinder, keeping x/D fixed. The corresponding effects are seen in the series of hydrogen-bubble photographs displayed in figure 9 for various control cylinder positions; the Reynolds number is 120 (the vortex street is not suppressed!) and $D/d = 7$. It is difficult to interpret the altered wake structure from these photographs, but some details will follow in §§6.2 and 6.3.

One consequence of the suppression of the vortex street is the concentration (compare figures 1 and 3) of the bulk of the momentum defect to a narrower region than in the natural case, and the corresponding enhancement of the maximum momentum defect. Figure 10 shows, at $x/D = 58$, mean velocity profiles with and without control. Repeated measurements have shown that the modified momentum defect behind the cylinder results in a net drag reduction above and beyond the increase owing to the presence of the control cylinder. It should be emphasized (see figure 10) that the velocity defect in the controlled case occurs close to the cylinder

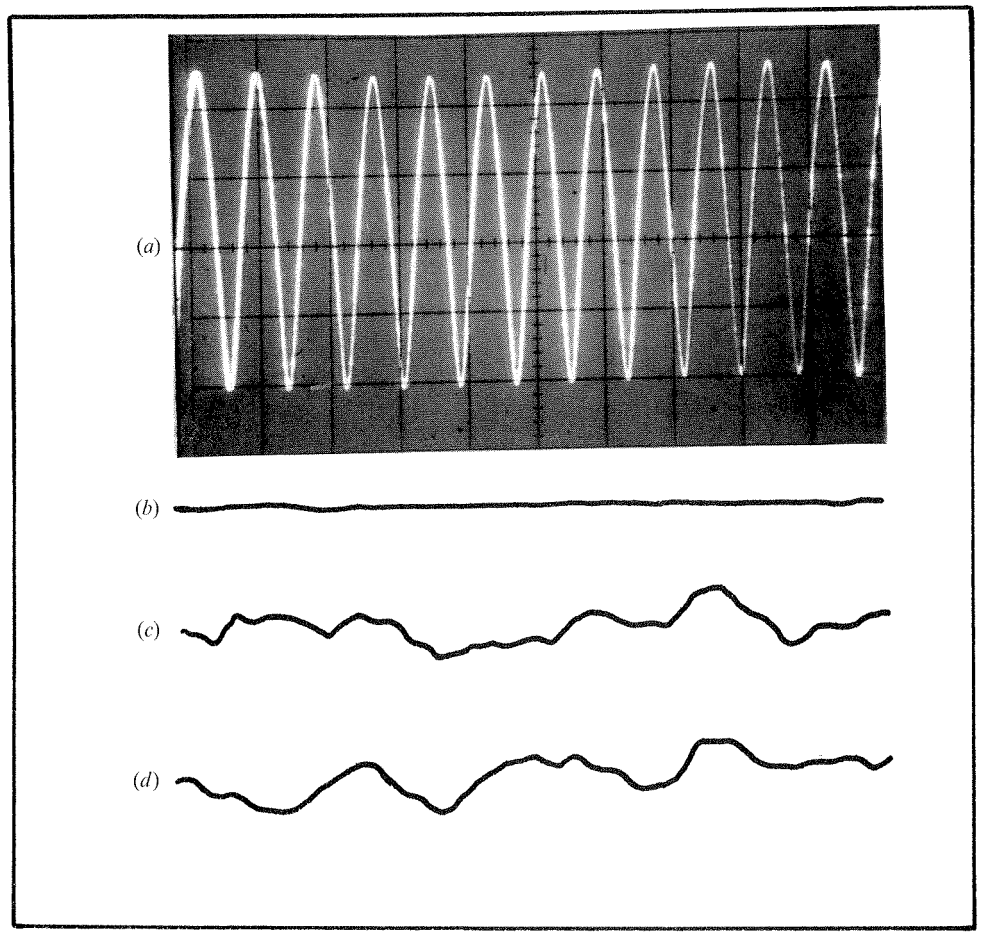

FIGURE 4. Hot-wire oscillations in the wake with and without control at $Re = 71$. (*a*) $x/D = 10$ and $y/D = 1$, no control; (*b*) $x/D = 10$ and $y/D = 1$, with control, $D/d = 11$; (*c*) same as (*b*), except for an amplification of about 20; (*d*) $x/D = 100$, all other conditions remaining the same as in (*c*). There is typically some small amplification of the disturbances between x/D of 10 and 100.

axis, and is accompanied by a weak overshoot (above the free-stream speed) occurring over a large width. This latter fact is especially important for a proper measurement of drag. (Only half profiles have been plotted in figure 10 to emphasize details but full profiles were indeed measured to obtain the drag.) Typically, for $Re = 80$, there is about a 20% reduction in the drag coefficient. Not all positions of the control cylinder accompanying the suppression of the vortex street decrease drag, and this aspect has been examined in some detail by Ahlborn & Lefrancois (1985).

3.2. *Influence of secondary parameters on the observed suppression*

The vortex street formation in the natural case depends on a variety of parameters such as the aspect ratio of the cylinder, the blockage ratio H/D (H is the tunnel dimension normal to the flow as well as the cylinder axis), three-dimensionalities and end conditions, and it is therefore to be expected that the control will also show some dependence on these parameters in addition to the diameter ratio D/d. On this last effect, we note that the vortex street can be suppressed to higher Reynolds numbers by increasing the relative size of the control cylinder, but we have not pushed this

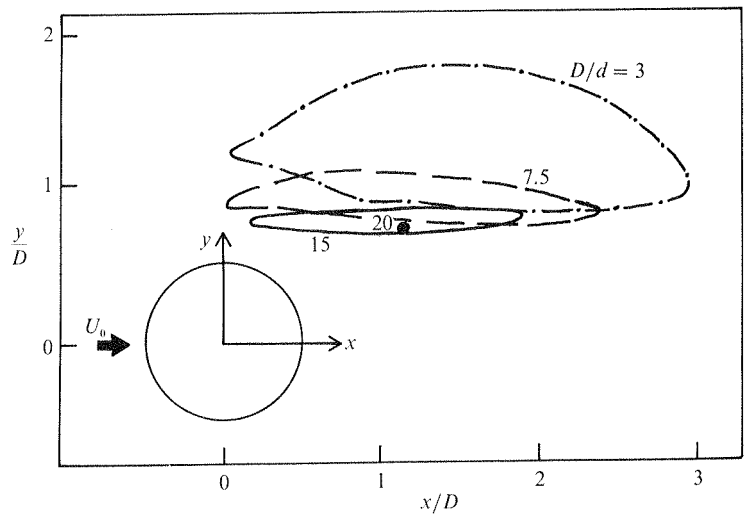

FIGURE 5. Regions of suppression for four values of D/d. These regions are symmetrical about the plane $y = 0$. $Re = 80$.

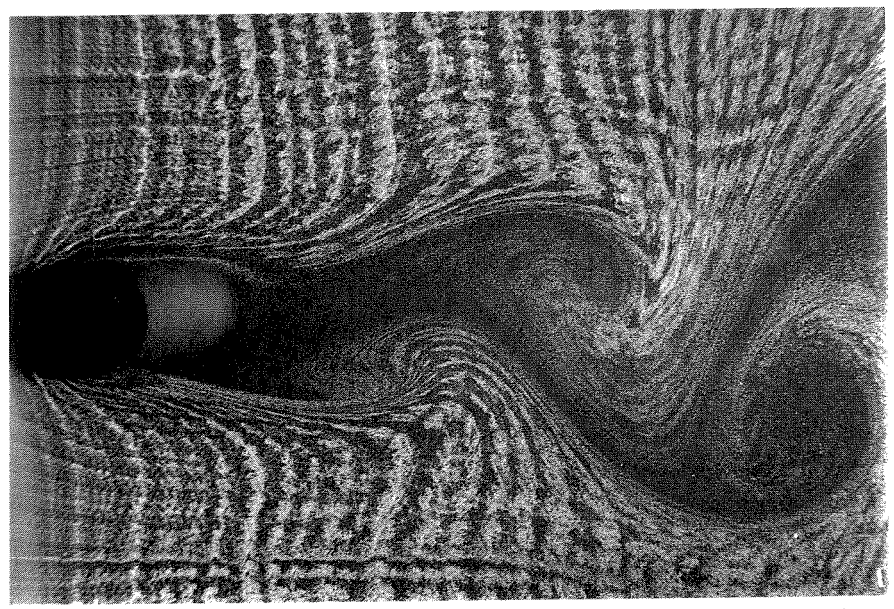

FIGURE 6. Details in the near field of the vortex shedding cylinder at $Re = 90$. No control is applied. The extent of the flow field is from x/D of 0 to 6.6.

to the limit because as $d/D \to 1$ (from below) it becomes increasingly difficult to argue that the flow behind a 'single' cylinder is being investigated. Here we briefly examine the influence of the rest of the parameters on the control phenomenon, but note that the study is not exhaustive in view of our emphasis on the basic phenomenon which does not depend on any of these parameters.

As described by Nishioka & Sato (1974), Mathis *et al.* (1984), Strykowski (1986) and Sreenivasan, Strykowski & Olinger (1986), the critical Reynolds number for natural vortex shedding behind cylinder increases when the ratio L/D is decreased.

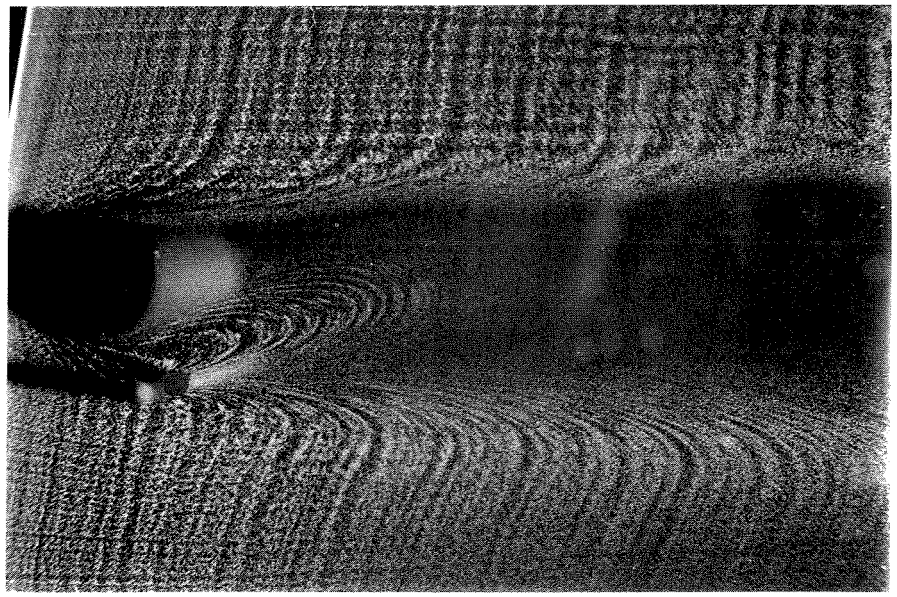

FIGURE 7. Complete suppression of vortex shedding at $Re = 90$, $D/d = 7$. The control cylinder is located at $x/D = 1.2$ and $y/D = 1$.

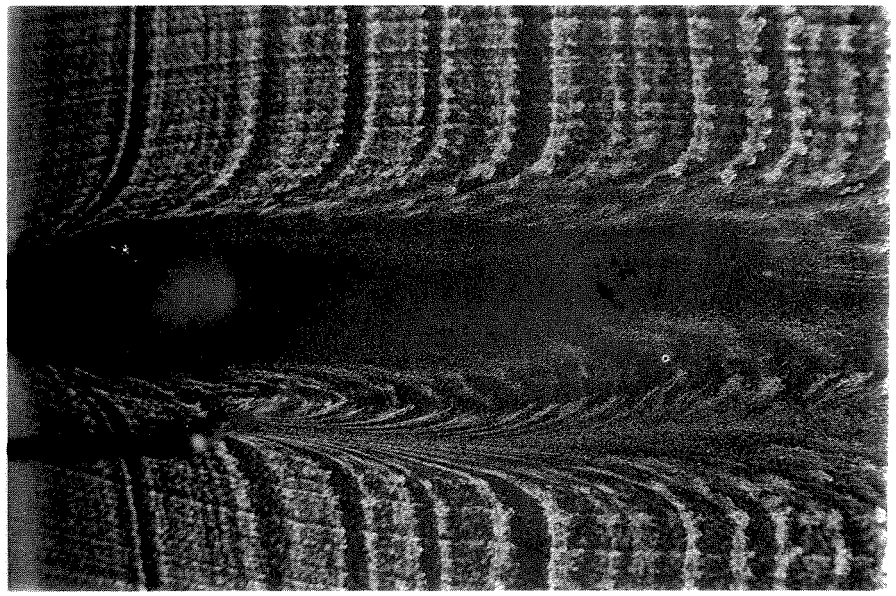

FIGURE 8. Complete suppression of vortex shedding at $Re = 90$, $D/d = 7$. The control cylinder is located at $x/D = 1.6$ and $y/D = 1.2$.

A similar effect has been documented by Shair *et al.* (1963) for the influence of the blockage ratio. In the present investigation three different facilities with different L/D and H/D were used, and the critical Reynolds numbers were correspondingly found to be somewhat different. For example, the natural critical Reynolds number in the water channel was about 60 ($L/D = 15$), but it was about 46 in both the wind

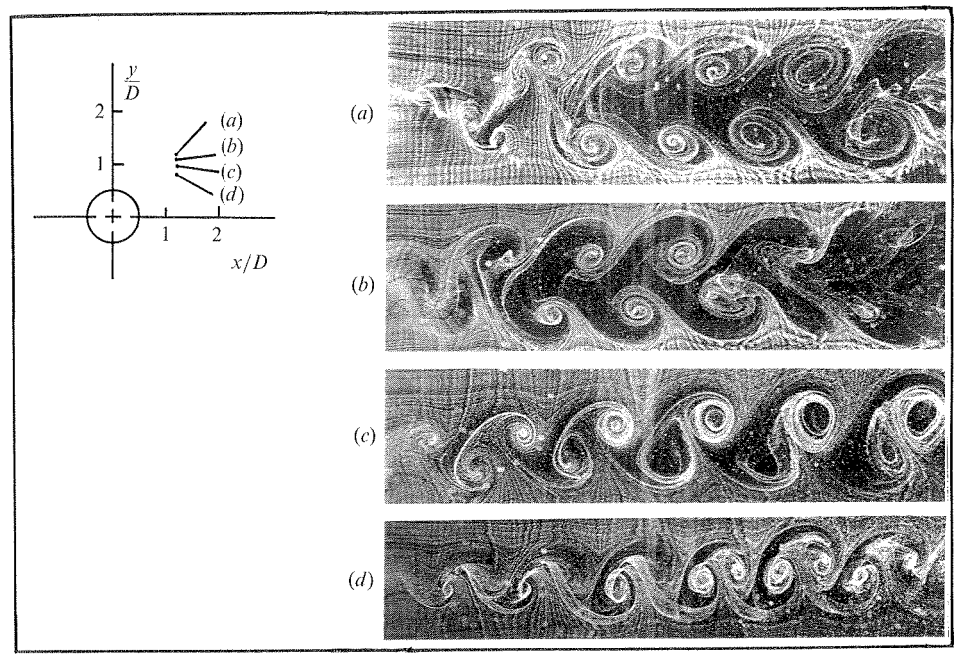

FIGURE 9. Hydrogen-bubble pictures showing the influence of the control cylinder at $Re = 120$, $D/d = 7$. The photographs extend from 8 to 35 cylinder diameters downstream of the main cylinder. The inset indicates the corresponding control cylinder positions.

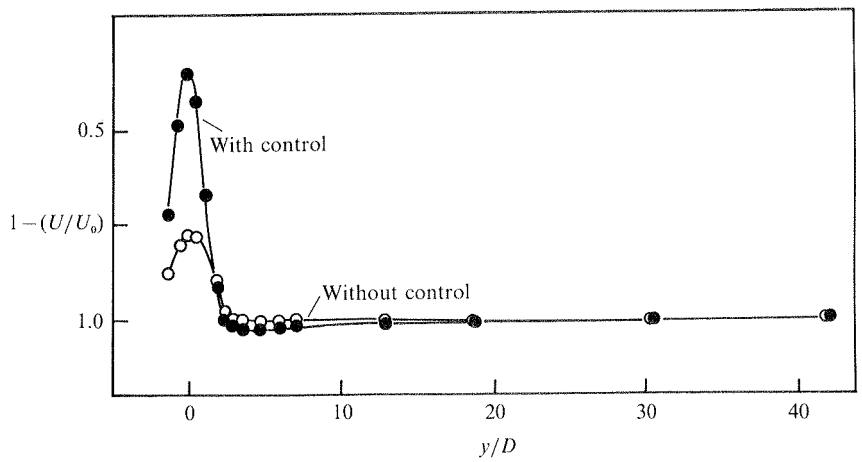

FIGURE 10. Mean velocity distribution $1-(U/U_0)$ at $x/D = 58$, $D/d = 8.5$ and $Re = 65$. Notice the long tail for the case with suppressed shedding.

tunnels ($L/D = 60$). It thus came as no surprise that vortex suppression was possible up to a Reynolds number of about 90 in the water channel, about 80 in the low-turbulence wind tunnel facility, and about 70 in the moderate-turbulence-level wind tunnel – all for the same diameter ratio D/d of 10.

It was determined by Sreenivasan *et al.* (1986) that the turbulence level affected the critical Reynolds number only marginally. We therefore believe that some of these differences are due to differences in end conditions and three-dimensionalities. For instance, in the low-turbulence tunnel, the test section was circular and the

tunnel walls were used as the end plates (consequently the control cylinder passed through the tunnel walls), while in the other case, the end walls artificially selected a part of a much longer cylinder.

While the precise details of the suppression phenomenon are sensitive to a variety of secondary parameters (such as the position of the control cylinder, aspect ratio of the main cylinder, the tunnel height to cylinder diameter ratio, turbulence level, etc.), it should be emphasized that the occurrence of the basic phenomenon is quite independent of such details (in some moderate range). It is precisely to establish this last fact that we undertook a numerical investigation of the two-dimensional wake, the results of which (see §4) have confirmed the experimental findings. For most experimental work to follow, we chose $D/d = 10$, $L/D = 60$ and $H/D = 60$ as being representative of the control of unconfined flow past a two-dimensional cylinder.

Some further remarks are appropriate. First, in an experiment with two symmetrically arranged control cylinders located at $x/D = 1.2$ and $y/D = \pm 1$, vortex street suppression was achieved up to a Reynolds number of about 100, compared to about 80 in the same apparatus for the single control cylinder case. This rules out the possibility that the observed suppression is a consequence of the asymmetry produced by the single control cylinder. For convenience in experiments, however, we have subsequently worked with a single control cylinder. Second, similar suppression was observed in the wake of other bluff bodies (see §5), including those with sharp edges facing the flow, thus ruling out the suggestion that possible movement of the separation 'point' might be responsible for the observed phenomenon. This also suggests that the important dynamical effect is associated with changes in the wake rather than with changes in the flow on the body itself. Finally, as already observed, the control cylinder did not have to produce its own vortex street to achieve suppression, thus eliminating the possibility that the phenomenon is related to some type of constructive or destructive interference with the vortex shedding behind the main cylinder.

We close this section by emphasizing that the vortex street suppression at some supercritical Reynolds number can be achieved either by bringing the cylinder into an appropriate position after the vortex shedding has started in the normal way, or by positioning the control cylinder in that same position prior to setting up the flow. In the former case the existing vortex patterns disappear, while in the latter case vortex shedding never appears. It is of fundamental interest to note that the final effects of both scenarios are the same in all respects measured here. It is this feature that will permit us to interpret the experiments from impulsively started flows as being relevant to steady-state vortex street formation. This is also the justification for the numerical calculations of impulsively started flows to be described in the next section.

3.3. *Frequency of vortex shedding in the controlled cases*

One way of quantifying the changes occurring in the wake is by monitoring the vortex shedding frequency. Figure 11 shows the dimensionless frequency fD^2/ν with and without the influence of the control cylinder. The data were taken in the low-turbulence wind tunnel with $D/d = 10$. For $46 < Re < 80$ the vortex street is totally suppressed, and there are no pure-frequency oscillations in the flow. For $Re > 80$ the presence of the control cylinder significantly reduces the frequency from its normal value. The frequency is reduced by approximately 30% at $Re = 80$. It may appear from here that the primary effect of the control cylinder is to postpone the onset of vortex shedding to a higher Reynolds number, but it will be shown later that the effect is somewhat more complex.

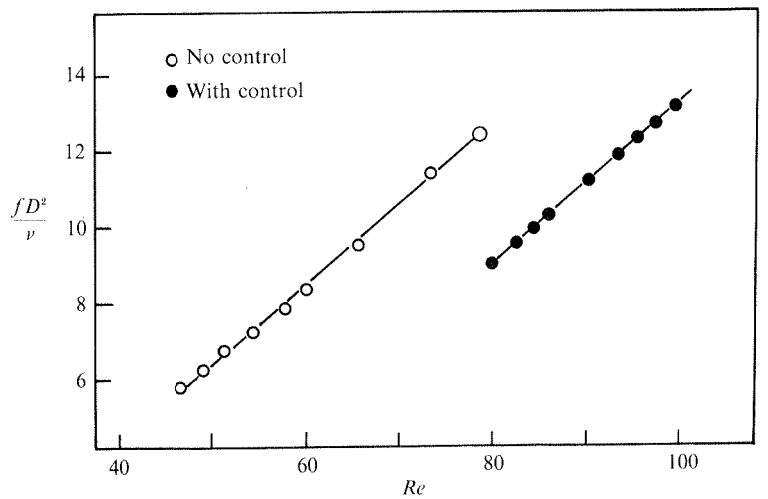

FIGURE 11. Dimensionless shedding frequency from the low-turbulence wind tunnel, with and without control. The control cylinder was located $x/D = 1.2$ and $y/D = 1$; $D/d = 10$.

4. Numerical simulations

4.1. *The motivation*

The smallness of the main cylinder (diameter on the order of 1 mm) necessitated by low-Reynolds-number flows in air prevented detailed measurements in the immediate neighbourhood of the cylinder; this limitation is compounded by the sensitivity of the near-wake region (closer than say 3.5 to 4 diameters) to insertion of hot-wire probes, and seeding problems with laser Doppler measurements make such measurements uncertain also. Computations could thus supplement experimental results. Secondly, the vorticity field is not obtainable in experiments, while it can be computed. As we shall see, this will be helpful for the interpretation of the results to be given in §7. Thirdly, the use of the full time-dependent numerical solution of the Navier–Stokes equations enables an accurate realization of the impulsively started flow which, in experiments, can only be simulated approximately over timescales smaller than a 100 ms. Finally, it was desirable to have an independent verification of the suppression phenomenon which, as discussed in §3, is sensitive in details to many secondary features. It was essential to establish that the basic phenomenon was not a consequence of some of the secondary features including small three-dimensional effects.

The results presented here are a part of an ongoing investigation of impulsively started flow past circular cylinders, the immediate goal being the confirmation of the experimental findings. Other details will be reported elsewhere. All computations were performed at the DFVLR in Göttingen.

4.2. *The numerical scheme*

The numerical technique applied to this problem was the finite-difference Galerkin method first developed by Stephens *et al.* (1984) for approximating the steady Navier–Stokes equations in two-dimensions. This technique has been modified here to approximate the full time-dependent Navier–Stokes equations through an explicit time-stepping scheme. This latter scheme has been implemented by Hannemann *et al.* (1985) for the driven cavity, and Hannemann & Oertel (1989) for the flow

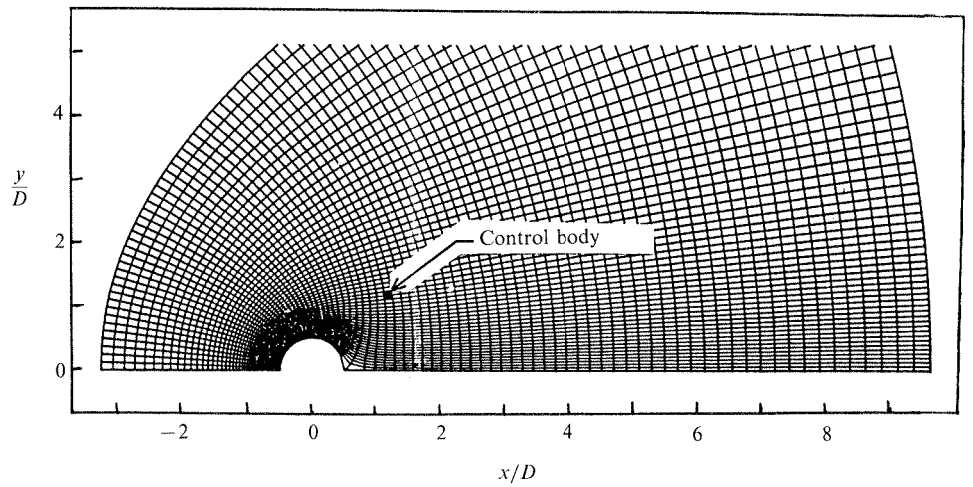

FIGURE 12. The computational grid for the numerical simulation.

behind a flat plate. Here, we provide only a brief description of the method, and refer the reader to the above references for details.

The principal advantage of the finite-difference Galerkin method is the elimination of the pressure from the equations of motion by projecting them into a divergence-free space. This simplification allows the boundary conditions to be prescribed entirely in terms of the velocity field, thus increasing the accuracy. Central differencing was used to eliminate artificial dissipation and false damping. For the present problem – where we require accurate time-dependent solutions of a flow field thought to be absolutely unstable (§§6 and 7) – the implementation of the simple no-slip boundary conditions on the body was essential. Furthermore, the technique has the advantage that it captures the wake instability naturally, i.e. the vortex street is developed without external forcing, a condition believed to be essential for analysing absolutely unstable flows. (In this method, the anti-symmetric numerical fluctuations begin to grow exponentially in time after the quasi-steady state is reached. Depending on the accuracy with which the equations are solved by the conjugate gradient method the exponential growth can be observed for up to eight orders of magnitude before the saturation state is reached; see Hannemann & Oertel 1989). This feature was lacking in many previous investigations, some exceptions being Hirota & Miyakoda (1965), Thoman & Szewczyk (1969), and Hannemann & Oertel (1989). Fixed potential flow boundary conditions were applied to all boundaries except the outflow where the curvature of the streamwise velocity was extrapolated to zero after each time-step; a fixed time-step equal to $0.001D/U_0$ was used throughout. Careful examination of the vorticity field revealed that the 'soft' outflow boundary conditions had an upstream influence on the order of one cylinder diameter.

The cylinder geometry was simulated using a transformation due to Fornberg (1980). The computational grid, shown in figure 12, concentrates grid points on the leading edge of the cylinder as well as in the wake region where finer resolution is required; the grid retains orthogonality in all regions. The present grid was the coarsest of those used by Fornberg but, as he pointed out, it has sufficient resolution for the Reynolds number of 55 being investigated here. Owing to computing

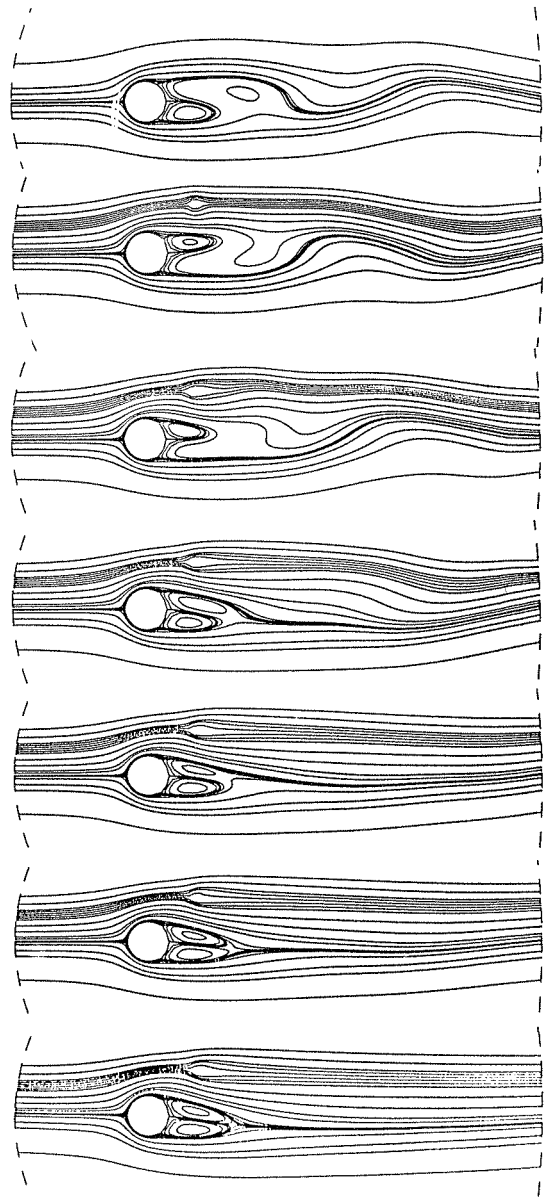

FIGURE 13. Instantaneous streamline pattern indicating the effect of the control cylinder at $Re = 55$. The uppermost figure represents the natural case at the same Reynolds numbers as the rest. The remaining figures correspond to increasing values of tU_0/D. The control 'cylinder' is located as indicated in figure 12.

limitations, a relatively small physical domain ($-3.4 < x/D < 9.7$) was used; this prohibits detailed quantitative comparison of the numerical data with experiment.

4.3. *The principal result*

The natural wake development was computed to the vortex shedding state, after which the control 'cylinder' was introduced. Sometimes, for economy, calculations

were started by introducing large-amplitude initial perturbations. The control 'cylinder' was simulated by forcing the streamwise and normal velocity components to vanish at six grid points located at $x/D = 1.2$ and $y/D = 1.2$ occupying an area of side equal to $\frac{1}{7}D$. Computations were continued in time up to the dimensionless time tU_0/D of 150 corresponding to 24 cycles of the vortex shedding oscillations. Approximately 20 CPU hours on a CRAY-XMP were required to reach this dimensionless time.

Figure 13 shows a sequence of streamline plots indicating the influence of the control 'cylinder' at various times during flow development. It is clear that the vortex 'street' is suppressed soon after inserting the control cylinder at tU_0/D of 0, leading to the formation of two standing eddies reminiscent of the subcritical state in the normal vortex shedding process. Further results will be given as appropriate in later sections.

5. Related experimental studies

5.1. *Experiments behind a flat plate facing the flow*

One of the important questions to be settled was whether the vortex street suppression by this method was peculiar only to the circular cylinder wakes. If it turned out that the same type of control can be exercised for flows behind other bodies which are different (e.g. with sharp edges facing the flow), the conclusion must be that the control becomes effective primarily by working on the wake rather than directly on the flow field on the body. For the problem of vortex shedding itself, Koch (1985) points out that it is not important which body produces the wake but rather the characteristics of the wake velocity profiles where the flow is approximately parallel. Triantafyllou & Karniadakis (1990) have recently shown that the vortex street can be generated numerically without the inclusion of the wake-producing body as long as the appropriate mean velocity profiles are incorporated into the simulation.

We chose a flat plate with sharp edges held normal to the flow. We applied the same control techniques using a single cylinder in one of the shear layer regions. The vortex shedding was suppressed in a similar fashion. For a control cylinder with a diameter equal to about a seventh of the flat plate height, suppression was attained up to a Reynolds number about 38% higher than the normal critical value. Because the separation points are fixed at the corners, this completely rules out the possibility that the suppression of vortex shedding is related to altering the location of the boundary-layer separation. The control cylinder could, however, affect the orientation of the layer at separation, a detail which requires further study.

5.2. *Heated control elements*

An interesting observation is that heating (in air) the control cylinder with direct current dramatically widens the region of suppression. The extent of enlargement of the suppression region can be seen by overlapping the contour in the cold control cylinder case with that corresponding to the heated control element (figure 14*a*) at about the same Reynolds number. The contour in the heated case corresponds to an estimated control cylinder temperature of 400 °C. Figure 14(*b*) shows that even at an Re of 120, there is a finite region in the wake where the heated control cylinder can produce vortex suppression. Even though the control contours are quite different from case to case, the most striking feature is that their downstream extent was never greater than about 4 diameters.

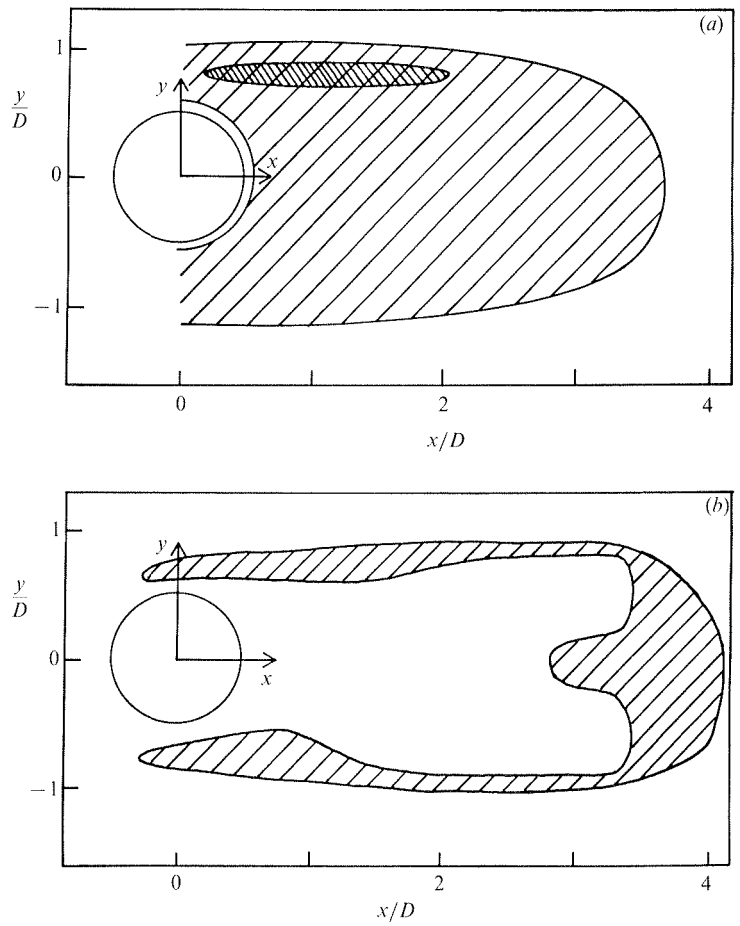

FIGURE 14. Hatched region represents the domain of vortex suppression using a control cylinder heated to about 400 °C with direct current. (*a*) $Re = 80$; (*b*) $Re = 120$. $D/d = 15$ in both cases. The cross-hatched region in (*a*) corresponds to the suppression domain with an unheated cylinder of the same dimensions.

6. Further measurements related to the physical explanation of the phenomenon

6.1. *Possible connection between vortex shedding and absolute instability*

Strykowski (1986) and Sreenivasan *et al.* (1986) argued that vortex shedding corresponds to the growth and saturation of disturbances which remain stationary with respect to the cylinder. Such flows have been called absolutely unstable, self-exciting or globally unstable (e.g. Koch 1985; Huerre & Monkewitz 1985; Bechart 1985; Triantafyllou *et al.* 1986; Monkewitz & Sohn 1986; Monkewitz & Nguyen 1987; Hannemann & Oertel 1989). Many of the measurements to follow are motivated to some extent by the view that absolute instability may have some bearing on the natural vortex shedding process. The following observations are relevant to this claim:

(*a*) The vortex shedding is dominated by a pure-frequency instability; the velocity spectral peaks are extremely sharp, and stand out about six to eight orders of magnitude above the background (Sreenivasan 1985). This is in contrast to the

instabilities in constant-density cold jets, boundary layers, etc., where similarly obtained spectral distributions possess a broad range of frequencies around the dominant peak, which itself is only an order of magnitude or so above the background noise. These instabilities are known to be of the convective type (Huerre & Monkewitz 1985), where perturbations travel as they are amplified. The main point is that travelling perturbations in spatially inhomogeneous flows cannot produce the pure-frequency phenomenon seen in wakes and variable-density jets (Sreenivasan, Raghu & Kyle 1989).

(*b*) The vortex shedding critical Reynolds number, as well as the saturation amplitude of the disturbance, are insensitive to the background noise or external forcing. This is in contrast to the instabilities in the other flows mentioned above, where the saturation amplitude of the disturbance is linearly proportional to its initial amplitude. This was shown by Sreenivasan *et al.* (1986).

(*c*) As shown by Strykowski (1986) and Sreenivasan *et al.* (1986), disturbances in the supercritical Reynolds number regime (that is, past the onset of vortex shedding) grow temporally, and at the same exponential growth rate everywhere in the flow; also see discussion below.

(*d*) The flow dynamics in the supercritical stage can be reasonably well described by the Landau–Stuart equation whose important constants are independent of space. For more precise and detailed discussion, see Strykowski (1986), Sreenivasan *et al.* (1986) and the independent work by Mathis *et al.* (1984) and Provansal, Mathis & Boyer (1987). The only way it appears necessary to incorporate the spatial dependence is via the spatial dependence of one of two of the complex constants whose ratio, however, remains independent of space.

These features support the notion that the mechanism leading to vortex shedding is governed by absolute instability. We hesitate to be more definitive simply because of the fact that the concepts are valid strictly for spatially homogeneous systems perturbed by an impulse-type response. In wakes behind objects we do not meet these criteria even loosely because the wavelength of the unstable perturbation is comparable to the region of inhomogeneity. A different way of describing the dynamical process leading to vortex shedding is via the temporal growth of a two-dimensional eigenfunction. Jackson (1987) has calculated the stability of such perturbations in the wake of a cylinder and found that the spatial eigenfunction of the disturbance was first amplified temporally at the Reynolds number usually measured to be the vortex shedding Reynolds number. A similar two-dimensional analysis of the cylinder wake was undertaken also by Zabib (1987) and by Hannemann & Oertel (1989) for the wake formed downstream of a flat plate.

If the vortex shedding process is due to temporal growth of a two-dimensional eigenfunction as Jackson visualizes, or is related to absolute instability, it is natural to ask whether the suppression of vortex shedding is associated with the damping of the appropriate temporal modes. To investigate the amplification or suppression of temporal modes it is necessary to design a transient experiment to directly measure the temporal growth or decay rate of the wake oscillations. We have performed such experiments in the presence of the control cylinder and have determined the extent to which temporal modes are damped (see §6.3). However, to gain a proper perspective of these measurements, it is necessary to outline the temporal amplification and decay rate measurements in the natural wake. This is done below.

6.2. *Temporal modes and the formation of vortex shedding*

Let us first concentrate on the growth rates of disturbances in the wake at some supercritical Reynolds number. The experiments needed to determine these growth rates must consist of abruptly setting the flow at the desired Reynolds number, and observing how the oscillations grow in time. If the disturbance (at any given position) amplifies exponentially as one expects to be the case initially, one can obtain the growth rate a_r from

$$u \sim \exp(at),\ a = a_r + ia_i. \tag{6.1}$$

The globe valve mentioned in §2.1.2 was opened suddenly, and the streamwise velocity signal at the chosen location within the wake was digitally recorded either by the hot wire or LDV. Linearization of hot-wire signals was done in some cases, but since this did not produce significant differences, many experiments were done without linearizing. To obviate unnecessary changes in the mass flow rate, and to improve the effective time constant for the rise time of the mean velocity, the flow rate was increased from a value slightly below Re_{cr} (where only background fluctuations were present) to the desired supercritical Reynolds number at which the oscillations selected by the flow begin to grow from the background.

A typical mean velocity change as well as an oscillogram of velocity fluctuations are given in figure 15. The accompanying flow Reynolds-number variation in the top trace is from 43 to 49, occurring on a timescale of the order of 200 ms. The bottom trace (*b*) shows the manner in which the oscillations in the streamwise velocity, measured at $x/D = 10$ and $y/D = 1$, grow with time. The signal in figure 15(*a*) was low-pass filtered below 30 Hz so as to reflect only the mean velocity variations, while the trace in figure 15(*b*) was high-pass filtered above 30 Hz to remove the mean velocity variation. The vortex shedding frequency was about 48 Hz, so that this high-pass filtering did not introduce too many phase or frequency modifications in the oscillations. The oscillations commence only after the Reynolds number attains the supercritical value; hence, it is clear that the characteristics of the oscillations correspond unambiguously to this supercritical state. This behaviour was observed even at those supercritical Reynolds numbers for which the characteristic growth time of the oscillations was comparable with or smaller than the rise time of the mean velocity. Presumably, oscillations do not amplify at the intermediate supercritical states because the instability associated with such transient states does not have time to develop.

The amplitude of the envelope in figure 15(*b*) can now be processed to obtain the growth rate a_r in (6.1) at the Reynolds number corresponding to the upper plateau in figure 15(*a*). LDV measurements made at 5 diameters downstream of the cylinder show exactly the same features. All growth rate measurements were made in the shear-layer region of the wake (that is, the region in which only one frequency is apparent in the hot-wire or LDV signal). Measurements at different streamwise positions did not show differences in growth rates.

While the measurement of growth rates is relatively straightforward, the same cannot be said of decay rates. In determining growth rates, we set the flow instantly (in principle) to the required supercritical Reynolds number starting from some subcritical state. Since the latter does not possess any preferentially periodic oscillations, the flow is free to choose the frequency and amplitudes appropriate to the supercritical Reynolds number. In contrast, decay measurements require the examination of the wake response in the subcritical state, where periodic oscillations

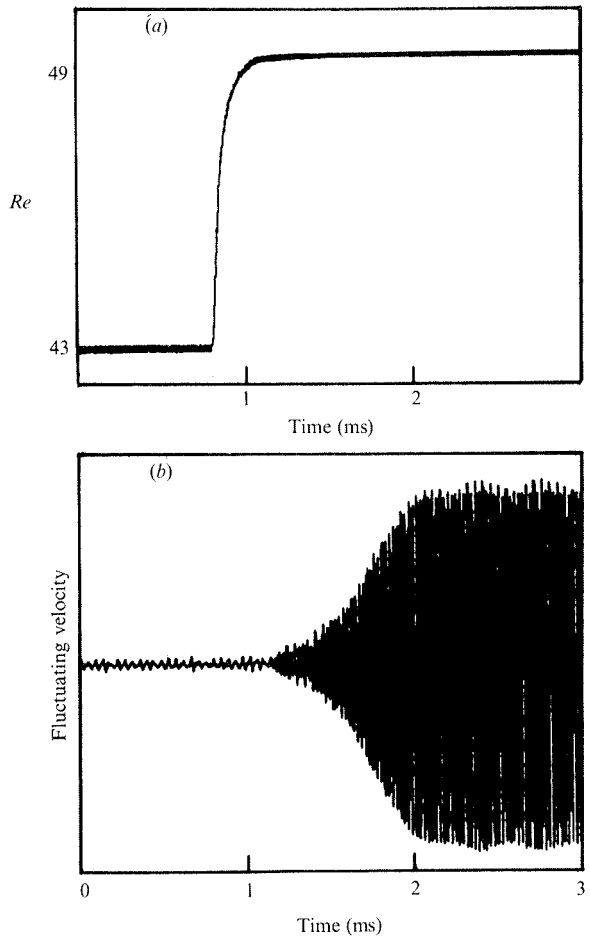

FIGURE 15. Simultaneous records of the mean and fluctuating velocities. The flow Reynolds number was increased from 43 to 49 (the critical Reynolds number, Re_{cr}, being 46 in this instance). Trace (a) was low-pass filtered below 30 Hz, and trace (b) was high-pass filtered above 30 Hz.

can be established only by means of some external forcing. The correct procedure would therefore be to establish (by some external means) flow oscillations at the right frequency appropriate to the desired subcritical Reynolds number, and switch off the forcing to quantify the ensuing decay of the oscillations. One does not know *a priori* what this right forcing frequency should be (or, for that matter, whether such a frequency exists), and how the decay rates depend on this frequency. We have addressed these issues at some length and will report them in detail in a forthcoming paper (preliminary results appeared in Sreenivasan *et al.* 1986), but note for present purposes that the decay rates are essentially invariant with the precise excitation frequency or the method in which the forcing was accomplished. The primary point is that the decay rates of wake oscillations were observed to be exponential in all cases (see figure 16 for an example), and the coefficient a_r in equation (6.1) was obtained as for the growth case – the difference, of course, being that a_r is negative during decay.

The measured growth and decay rates taken in the cylinder wake without the presence of a control cylinder are collected in figure 17. (The reason for normalizing

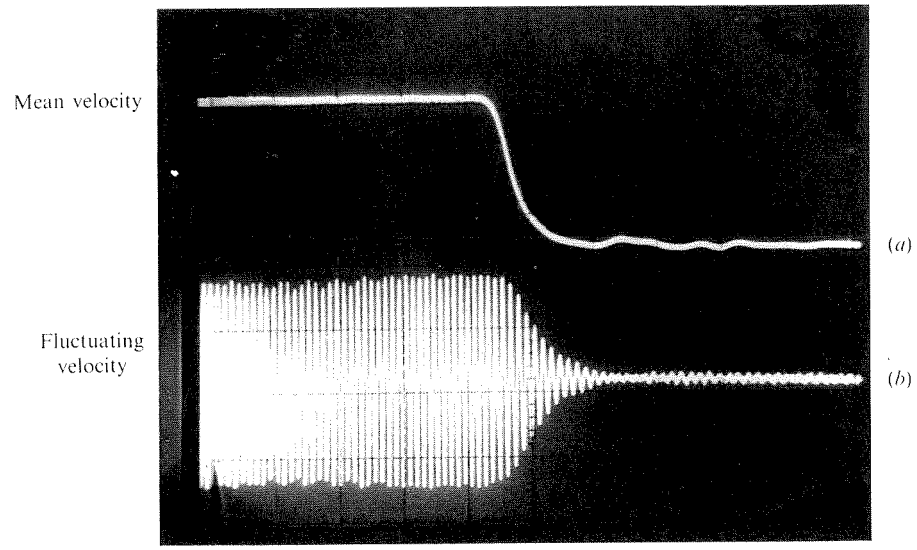

FIGURE 16. Mean and fluctuating velocity response, measured during decay. The flow Reynolds number is reduced from 50 to 44. The signal was recorded from a hot wire located at $x/D = 10$ and $y/D = 1$; $Re_{cr} = 46$.

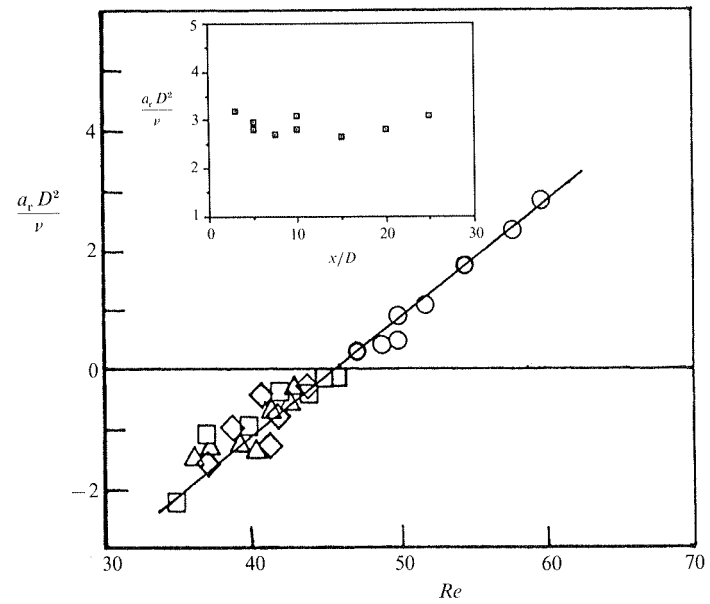

FIGURE 17. Amplification and decay rate measurements taken for a variety of conditions and by different experimental methods briefly described in the text. For details, see Sreenivasan *et al.* (1986). Cylinder aspect ratio = 60. The critical Reynolds number corresponding to zero growth rates is 46. The inset shows growth rate measurements made at different streamwise positions in the wake shear layer at $Re = 60$.

the growth and decay rate data in figure 17 by the viscous time scale D^2/ν instead of the convective time scale D/U_0 is simply that $a_r D^2/\nu$ is usually of the order unity while $a_r D/U_0$, which is smaller by the factor of the Reynolds number, gives numerical values on the order of 0.01.) Only one set of growth rate data has been

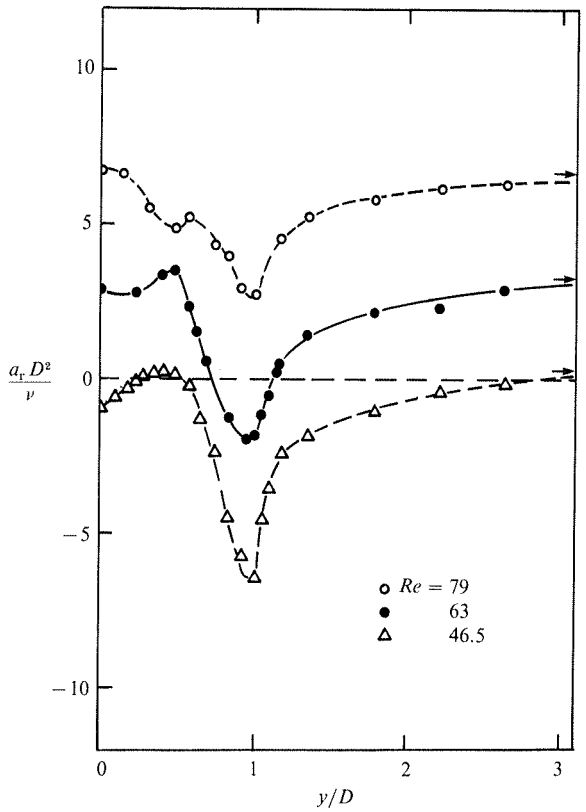

FIGURE 18. Amplification and decay rates measured in the wake for various control cylinder positions at $Re = 79$, 63 and 46.5. The control cylinder is traversed along the plane $x/D = 1.2$; $D/d = 10$. The arrows indicate the asymptotic values of a_r occurring when the control cylinder is completely removed.

plotted, but other sets obtained at different x/D (by LDV as well as hot wires) were no different (see inset to figure 17), except that the measurement uncertainty was greater at larger downstream distances, both because of the smaller amplitudes and somewhat higher three-dimensional effects there.

Oscillations grow rather slowly in the very close positive vicinity of Re_{cr}; it is exciting to watch sustained oscillations appear just above Re_{cr}, say $Re_{cr}+0.1$. The growth rates there are so small that saturation amplitudes are reached only for long times of the order of a minute corresponding to about 10^4 convective timescales D/U_0. Many flow facilities do not have test sections that are 10^4 cylinder diameters long, and it is therefore clear that the appearance of sustained pure-frequency oscillations at these Reynolds numbers cannot be related to any spatial development in the flow. In a few cases, we observed the growth phase extending for over one minute followed by an immediate decay over a comparable period of time, apparently because the Reynolds number had inadvertently fallen from just above to just below Re_{cr}.

6.3. *Control by suppressing temporal modes*

From the above discussion it appears logical to expect that vortex shedding will be suppressed if the exponentially growing temporal disturbances are damped. To examine this picture, we have measured, as described above, the temporal growth

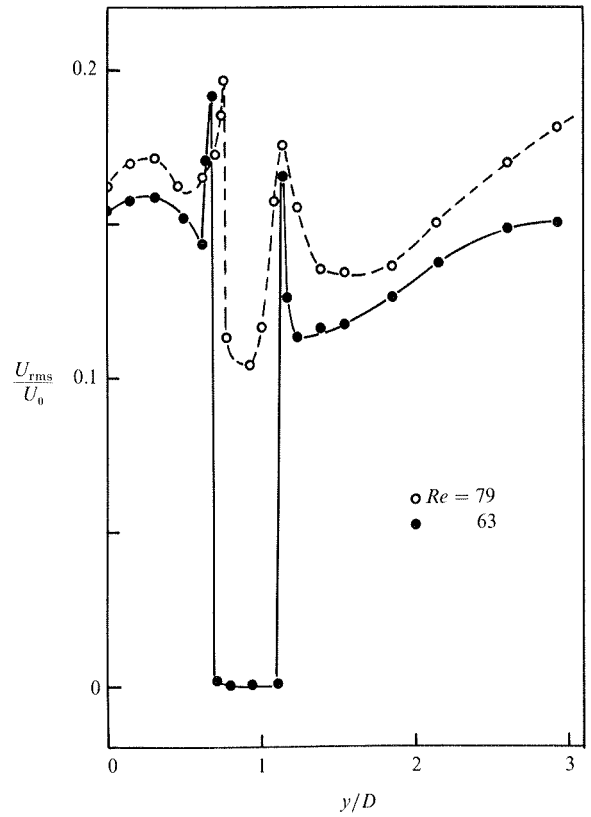

FIGURE 19. Magnitude of r.m.s. velocity fluctuations measured in the shear layer at $x/D = 8$, for various control cylinder positions. The control cylinder is traversed along the plane $x/D = 1.2$; $D/d = 10$.

and decay rates in the presence of the control cylinder. For a fixed streamwise position, $x/D = 1.2$, the control cylinder is traversed in the normal direction, all the way from very far (effectively corresponding to the control cylinder out of the flow domain) to the cylinder axis.

Measured values of a_r are given in figure 18 for $Re = 79$, 63 and 46.5 (that is, just above the critical Reynolds number in the natural case) as a function of the control cylinder position y/D. At $Re = 79$, the control cylinder reduces $a_r D^2/\nu$ from 6.7 to as low as 2.5, but the sign is not changed. In contrast, at $Re = 63$, the temporal instability is suppressed (i.e. $a_r < 0$) for control cylinder positions $0.7 < y/D < 1.1$.

The importance of this observation can be seen in figure 19, where the root-mean-square (r.m.s.) magnitude of the streamwise velocity fluctuations (in the asymptotic state) is plotted against the control cylinder position as before. The r.m.s. measurements were made by a hot wire fixed at $x/D = 8$ and $y/D = 1$, but their behaviour elsewhere is qualitatively the same. At $Re = 63$, the effectiveness of suppression is strikingly clear, precisely when the control cylinder is in the region $a_r < 0$. Visual observations confirm that the vortex street disappears for these conditions. This supports the view that the suppression of vortex shedding is related to the damping of some temporal instability in the frame of reference of the cylinder. At $Re = 79$, reduced growth rates result in reduced r.m.s. intensity but the control cylinder does not suppress the oscillations completely. Strykowski & Sreenivasan

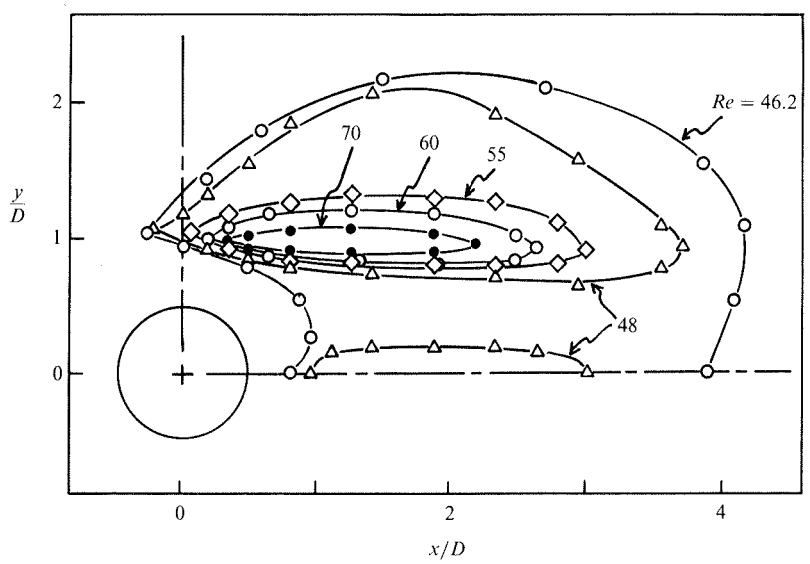

FIGURE 20. Contours where $a_r = 0$ for several Reynolds numbers. Data are symmetric about the line $y = 0$; $D/d = 10$.

(1985*b*) report that the effect of the control cylinder in both cases pervades for streamwise distances of the order of 100 diameters.

The r.m.s. velocity pattern shown in figure 19 is generally consistent with the growth rate data of figure 18 and a related observation made by Strykowski (1986) and Sreenivasan *et al.* (1986) that smaller saturation amplitudes must accompany smaller growth rates. The exception is in the neighbourhood of $a_r = 0$, where the amplitude rises sharply, as seen in figure 19. This repeatable phenomenon has no satisfactory explanation. Flow visualization in a water channel shows that complex spatial changes accompany such transitions, and the jump in the single-point r.m.s. measurements offer no help in understanding them.

The features observed in figure 18 at $Re = 79$ and 63 occur also at $Re = 46.5$ (remembering that $Re_{cr} = 46$ in this apparatus); vortex street formation is suppressed except when the control cylinder is located in the region $0.25 < y/D < 0.5$, and $y/D > 2.8$. Oscillations do appear for these two cases, but the saturation amplitude is small, and is not reached until several seconds after the flow is set up because a_r is very small. We define from figure 18 an 'optimum' position for the control cylinder corresponding to the most negative growth rate; this occurs at approximately a $y/D = 0.95$.

An instructive representation of the influence of the control cylinder is to present the locus of all points in the (x,y)-plane corresponding to $a_r = 0$ for different Reynolds numbers (figure 20); as anticipated in §3, the boundaries in figure 20 correspond quite well to those of figure 5. As the Reynolds number is increased, one reaches a value at which the contour shrinks to a point. At this point, the control cylinder position becomes very critical, and suppression at higher Reynolds number is not possible.

An interesting point is that, at the Reynolds number of 48, there is a finite region on and around the wake centreline within which the control cylinder can suppress shedding. At a Reynolds number just above the critical value of 46 (nominally 46.2), the suppression region becomes contiguous and wide, consistent with the growth rate

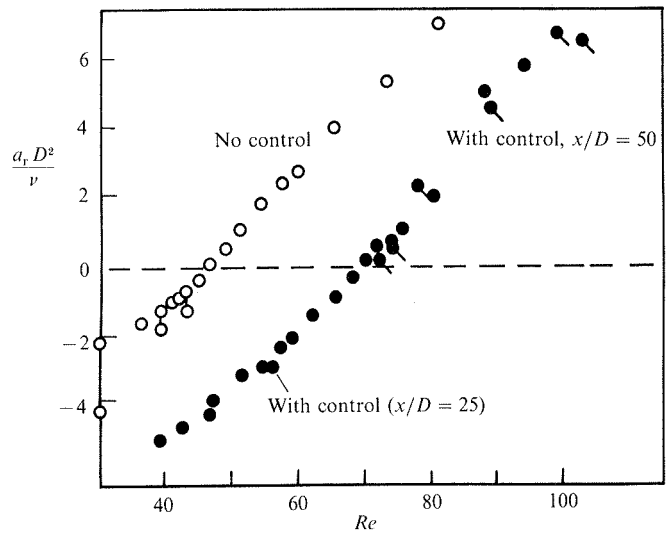

FIGURE 21. Amplification and decay rates in the wake with and without control. The control cylinder was located at $x/D = 1.2$ and $y/D = 0.95$; $D/d = 10$.

data of figure 18. Notice that the shape and extent of the suppression region is similar to that at the higher Reynolds numbers in the case of a heated control cylinder (see contours for $Re = 80$ in figure 14*a*). However, we did not observe a contour similar to figure 14(*b*) with an unheated control cylinder, indicating that comparisons between the two phenomenon must be made with some discretion. There is little doubt that the heated wake problem is rich in detail and deserving of further study; such an effort is in fact currently under way.

In the above experiments, we have varied the control cylinder position keeping the flow Reynolds number fixed. Alternatively, one can keep the position of the control cylinder fixed, and vary the Reynolds number starting from the steady state. (It is important to vary the flow speed slowly, just as it is important to vary the control cylinder position slowly, to avoid hysteresis effects.) The interesting point is that the two methods yield identical results, and more on this will be said in §7.

Figure 20 suggests that the critical Reynolds number in the presence of the control cylinder is never smaller than the natural value. That is, there is never a situation when the control cylinder ($D/d = 10$) induces instability in otherwise stable circumstances. This was checked carefully by fixing the flow Reynolds number at 46 and moving the control cylinder throughout the flow domain. Owing to geometric constraints in the wind-tunnel apparatus, the control cylinder could not be moved upstream of the plane $x/D = -0.5$.

By positioning the control cylinder at the limiting 'optimum' location of figure 18 ($x/D = 1.2$, $y/D = 0.95$), we have measured the temporal amplification and decay rates as a function of Reynolds number. The data are given in figure 21, which also shows that the growth and decay rates fall on a continuous line. As in the natural vortex shedding case, these were independent of the position of measurement. The comparison of the growth and decay rates with and without control shows that the influence of the control cylinder is to shift the curve by an approximately constant amount, very reminiscent of the frequency data of figure 11. The critical Reynolds

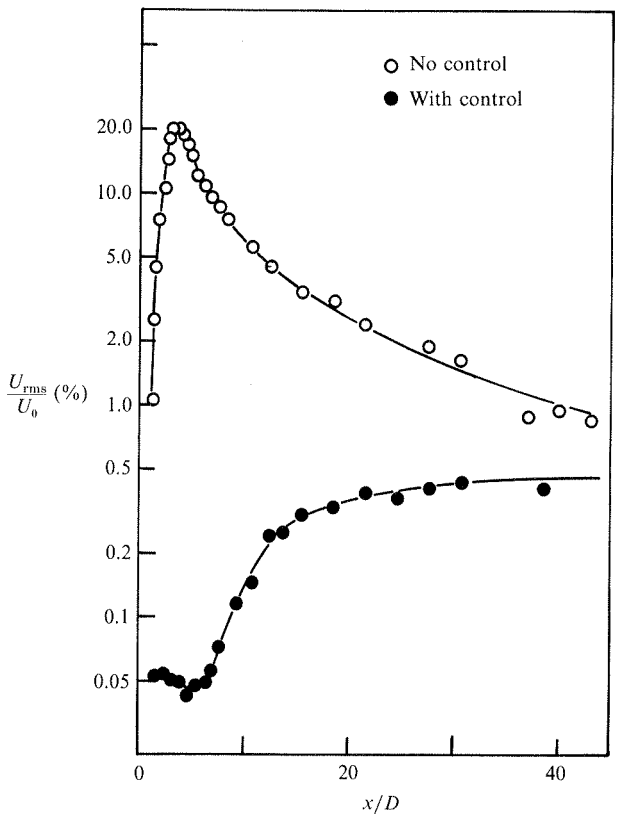

FIGURE 22. Root-mean-square streamwise velocity fluctuation with and without control, $Re = 78$. The control cylinder is located at $x/D = 1.2$ and $y/D = 0.9$; $D/d = 10$. The hot wire is traversed along the plane $y/D = 0.7$.

number, corresponding to $a_r = 0$, is about 70 in this flow apparatus; below Re of 70 the temporal instability and vortex street are simultaneously suppressed.

We envision that disturbances which 'stay put' (that is, have zero group velocity) as they grow in time eventually lead to vortex shedding. The phenomenon can be modelled as a 'self-excited oscillator' (see Olinger & Sreenivasan 1988*a*, *b*; Monkewitz 1988) which dominates the flow development. It is likely that the convectively growing instabilities of the type studied by Nishioka & Sato (1978) may exist underneath the basic structure of the temporally growing disturbances. These are normally masked by the overwhelmingly large temporal instabilities. By introducing the control cylinder and 'turning off' the temporally growing perturbations, the only possible instabilities now are of the convective type which convect downstream as they amplify, and therefore do not remain long enough in the vicinity of the cylinder to cause vortex shedding.

To examine this view further, we have presented in figure 22 the streamwise development of the r.m.s. velocity with and without control. In the natural wake, large saturation amplitudes peak with a distance of $x/D < 3.5$, and decay thereafter. The implication is that the wake environment beyond about x/D of 3.5 is stabilizing for these perturbations. These data are in reasonable agreement with those of Nishioka & Sato (1978). In contrast, the amplitude in the controlled case is two

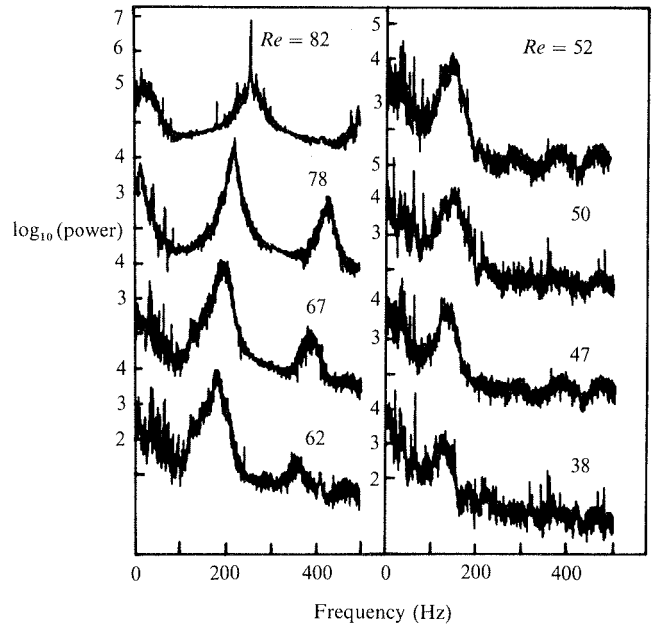

FIGURE 23. Power spectral densities of the streamwise velocity fluctuation at several different Reynolds numbers with the control cylinder located at $x/D = 1.2$ and $y/D = 0.95$; $D/d = 10$.

orders of magnitude lower in the near-wake region. The amplitude increases spatially downstream, reaching a peak around an x/D of 40, after which it decays (not plotted). As we shall see in the next section, the spectral composition of these latter fluctuations is broadband, this being a property of convectively unstable disturbances.

6.4. *Power spectral measurements*

The measurements presented are for the double-contraction wind tunnel with low-turbulence level in which suppression was possible up to a Reynolds number of about 80 (as against 70 in the single-contraction wind tunnel), for $D/d = 10$.

The power spectra in figure 23 outline the changes occurring as the Reynolds number is reduced from above to below 80. The control cylinder was located at the 'optimum' position, and the power spectra were recorded by a hot wire located at $x/D = 50$ and $y/D = 1$. For $Re = 82$, the wake is dominated by a pure frequency of high quality, several orders of magnitude above the noise level. (Closer to the cylinder, the spectral peak is even sharper and larger in magnitude, but we have chosen to measure far enough downstream to avoid possible asymmetry effects.) The spectral peak becomes considerably broader at $Re = 78$ with the maximum power level being reduced by over two orders of magnitude. The power spectra in figure 23 at $Re = 82$ and 78 would correspond roughly to the flows of figures 1 and 3 respectively. (The flow visualization in figure 3 is consistent with small downstream growth of disturbances which, however, do not seem capable of organizing themselves into periodic structures with sharp spectral peaks.) As described in §§6.3 and 7 the control cylinder eliminates the growth of the temporal mode (eliminating the associated large saturation amplitudes) but has relatively little influence on the small-amplitude spatially unstable disturbances (instabilities having positive group velocities).

The erosion of the peak as we decrease the Reynolds number appears continuous,

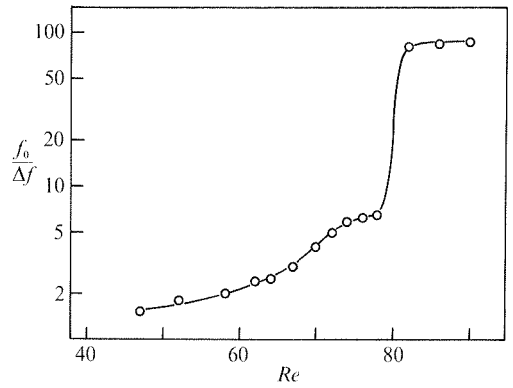

FIGURE 24. The quality $Q = f_0/\Delta f$ of the peak frequency in the power spectra from figure 23. Δf is measured at a power level two orders of magnitude below the peak value.

but the relative changes are not gradual. The abruptness of this transition can be quantified by measuring the quality $Q = f_0/\Delta f$ of the spectral peak, where f_0 is the frequency of the largest peak, and Δf is defined for present purposes as the frequency band measured at a power level two orders of magnitude below f_0. (Note that the usual choice of Δf corresponding to the $\frac{1}{2}$-peak power level would be uninformative here, besides resulting in a large scatter owing to the small values of Δf.) The quality is reduced by approximately two orders of magnitude (figure 24) in the narrow range of Reynolds numbers just bordering the 'critical' value. (Another quantity that shows a sudden qualitative change across the suppression contour is the dimension of the attractor in phase space. A detailed discussion of this matter would take too much space and is not central to the issue being discussed, but it is thought that the main result may be of interest to some readers. The so-called correlation dimension, evaluated according to an algorithm due to Grassberger & Procaccia (1983), was unity outside the suppression region, while it was unmeasurably high inside of them. This is consistent with the notion (Sreenivasan 1986) that the concept of the dimension of the attractor is not very useful in convectively unstable flows.)

One can also do the complementary experiment of keeping the Reynolds number fixed, and varying the control cylinder position. In figure 18, it was found that the temporal amplification rate became negative for a range of cylinder positions ($0.7 < y/D < 1.1$) at $Re = 63$. Figures 25(a–g) outlines the spectral changes for control cylinder positions varied across this region for a slightly different Reynolds number of 65; the inset roughly shows the various control cylinder positions with respect to the boundary between positive and negative growth rates. When the control cylinder is placed such that $a_r > 0$, spectral peaks are sharp (figures 25a and 25g), whereas in the immediate vicinity of $a_r < 0$ (figures 25b and 25f), the peak is much less dominant. In the centre of the contour corresponding to the 'optimum' control position (see inset), the growth rates are most negative and the power spectrum is most broad. An additional feature seen in figure 25, and to a lesser extent also in figure 23, is that the amplified disturbances are skewed to higher frequencies when the growth rate first become negative, and become symmetric only when it is reduced further. Strykowski (1986) has given an argument to show that this behaviour is consistent with expectations that a convectively unstable flow has set in.

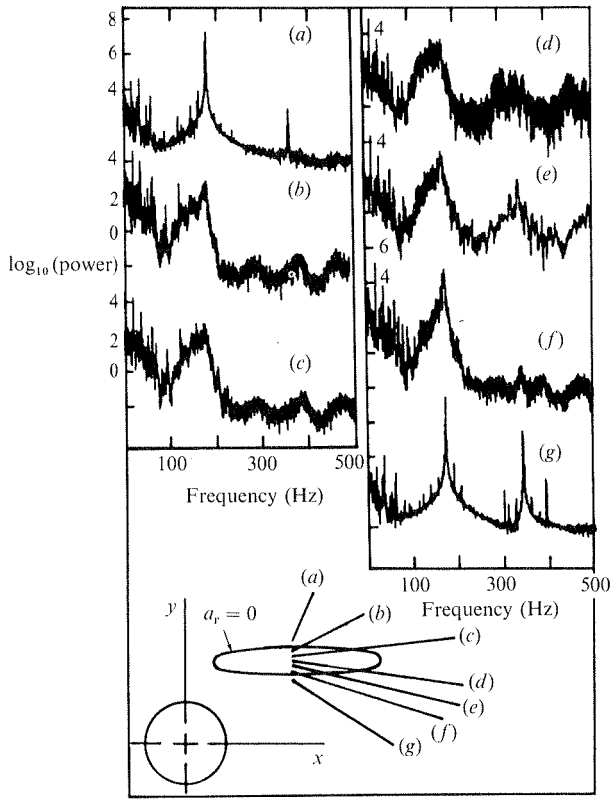

FIGURE 25. Power spectra of the streamwise velocity fluctuation at $Re = 65$ for various cylinder positions shown in the inset. The control cylinder was located on the plane $x/D = 1.2$; $D/d = 10$.

7. Discussion and conclusions

As mentioned earlier, the 'control' phenomenon is most likely to be related to changes occurring in the neighbourhood of the vortex shedding cylinder. It is our premise that the understanding of this 'control' will lead to an improved understanding of the vortex shedding itself. Here, we try to connect the various observations in a unified way. It is useful first to recapitulate the special features of this phenomenon, because it is in these features that the key to the explanation must lie.

7.1. *Special features of the present suppression method*

The first point is that, while some detailed aspects of the suppression phenomenon might be sensitive to three-dimensionalities, specific end conditions, free-stream turbulence level, etc., the essentials of the phenomenon are independent of them (as long as they are moderate). Strong evidence for the latter part of this statement comes from numerical calculations for an ideal two-dimensional case which showed features completely consistent with experiments in nominally two-dimensional flows. It is also clear that the control is possible only when the near field is manipulated in some way; recall that the control cylinder was not effective when placed downstream of x/D of 4. We infer that the vortex shedding phenomenon must be associated with the near field dynamics. It is also clear that the effect is not one of setting up an asymmetry, because two control cylinders are more effective than a single one.

Suppression by this technique is possible behind a variety of objects, and therefore the control cylinder effect is not one of altering the flow field on the body, such as moving the separation 'point'. This suggests that the vortex shedding itself is a process independent of the body, and is likely to be the property of its wake. Since we have already excluded unsteady effects as being unimportant for control, we infer also that the property of the mean velocity distribution in the wake is the most significant aspect determining the vortex shedding. The related numerical study of Triantafyllou & Karniadakis (1989) appears to confirm this conclusion. The problem of vortex shedding thus properly belongs to the realm of instability analysis.

Another important observation is that the suppression is not a dynamic effect resulting from some type of interaction between the unsteady flow field of the vortex shedding and the control cylinder. A point in favour of this view is that suppression at a given low Reynolds number above the critical value is achieved equally well either by bringing the cylinder into an appropriate position after the vortex shedding has started in the normal way, or by positioning the cylinder in that same position prior to setting up the flow. In the former case the existing vortex patterns disappear, while in the latter case vortex shedding is banished from appearing. It is of fundamental interest to note that the final effects of both scenarios are the same. It is in fact this feature that allowed us to interpret the experiments from impulsively started flows as being relevant to steady-state vortex street formation.

An intriguing property of the vortex shedding is that the spectral density of the velocity fluctuations in the wake possess high-quality peaks (Sreenivasan 1985; Sreenivasan *et al.* 1989), quite different in character from those of many other unstable flows. This pure-frequency oscillation has led to expectations that the instability is 'global' in nature or equivalently one in which the flow as a whole participates. Another related view is that the nature of instability is of the absolute type.

7.2. *Physical interpretation of the mechanism of vortex street suppression*

It is useful to recapitulate first the essential physics of vortex shedding itself. At low Reynolds numbers, the vorticity pumped into the wake from the boundary layers on the cylinder can be diffused away from the shear layer surfaces merely by viscous action. The classical view is that, as the flow Reynolds number increases, viscous diffusion alone cannot keep up with the increased vorticity production in the upstream boundary layers, and vortices break away at regular intervals, constituting 'vortex shedding.'

Let us briefly review the importance of the vorticity distribution and circulation in the wake shear layer to the formation of the natural 'vortex street.' As pointed out by Abernathy & Kronauer (1961) it is *not* necessary to have a wake-producing body to form a 'vortex-street.' The body is necessary to generate the shear layers, of course, but the main point is that it is the interaction of the shear layers, independent of the body, which forms the 'vortex-street.' A direct consequence is that it is not the reduction in base pressure which forms the 'vortex-street' but the formation of the 'vortex street' through shear layer interaction which results in a decrease in the base pressure. Further, by modelling the wake shear layers as vortex sheets – which is justified if the disturbance wavelength is large compared with the shear-layer thickness, as was found by Fage & Johansen (1927) – Abernathy & Kronauer found that the 'vortex street' formation was then only a function of the magnitude of the circulation in the shear layer and the shear layer spacing. (We temper this conclusion somewhat by noting that the existence of a growing antisymmetric perturbation for two parallel shear layers need not imply a nonlinear,

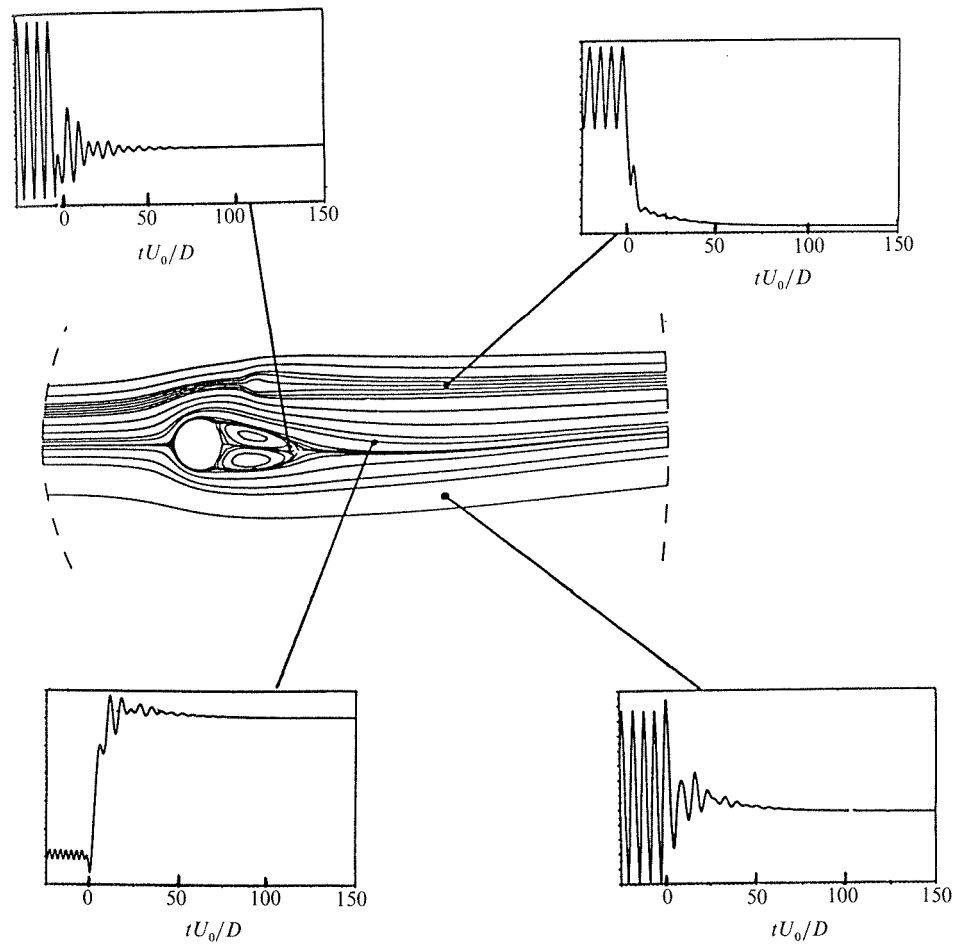

FIGURE 26. Velocity signals recorded at several locations in the flow field showing the suppression of vortex shedding at $Re = 55$. The control body is introduced at $x/D = 1.2$, $y/D = 1.2$ (see figure 12) at $tU_0/D = 0$.

single frequency entity, and it remains to be shown that the latter does not require the body.)

These results are qualitatively supported by Gerrard (1966) who described the 'vortex street' formation to be a function of the 'diffusion length' and 'formation length.' Gerrard's model predicts that the circulation in the shear layer must be of a sufficient magnitude before one shear layer draws the other across the wake centre plane. Further, this interaction must take place before a critical distance (formation length) is reached. In Gerrard's terminology the 'vortex street' could be inhibited if either the shear layer vorticity distribution was diffused (over a critical diffusion length) or the shear layers were prevented from interaction (over a critical formation length), the essential point being that the spreading of the shear layer means that only a part of it is drawn across to the other side.

We now recall some observations made in the control case. First, we showed in figures 6, 7 and 8 that a small amount of fluid is apparently diverted into the near-wake region from the free stream, although to widely varying extents depending on the precise position of the control cylinder. Although no quantitative information

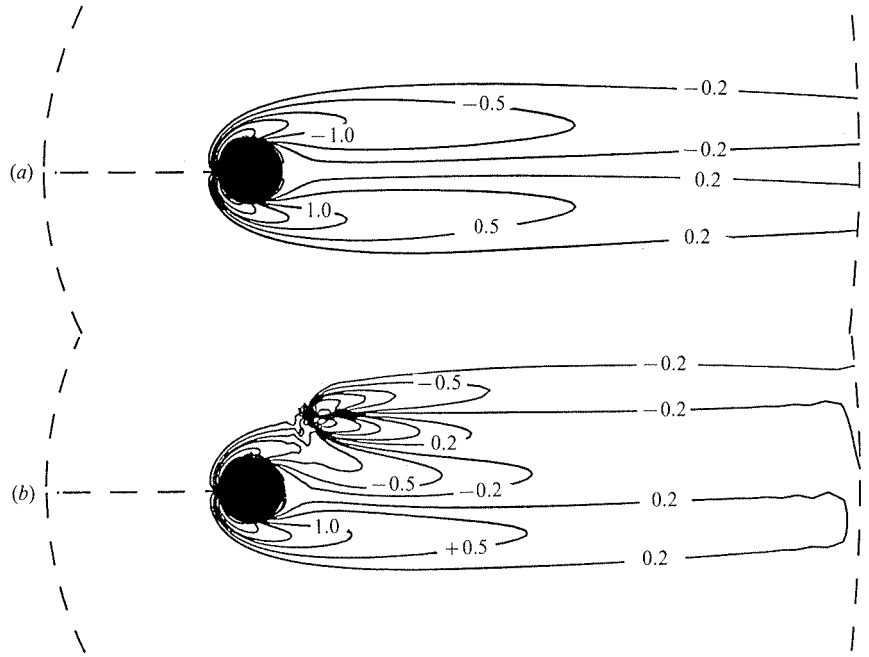

FIGURE 27. Mean vorticity contours at $Re = 55$ for the flow (a) without the control cylinder (quasi-steady solution) and (b) with the control cylinder ($tU_0/D = 150$).

was obtained in numerical investigations (§4) (computations were restricted to obtaining some basic quantities mainly because of the expense), the results were qualitatively consistent with this conclusion. For instance, the velocity–time trace to the lower left of figure 26 shows a substantial increase in the region behind the main cylinder whereas a sizeable velocity reduction occurs directly downstream of the control cylinder (upper right trace).

One must expect fluid diversion and the vorticity redistribution to be related. The numerically generated vorticity fields with and without the presence of the control cylinder (figure 27) show that the properly placed control 'body' redistributes vorticity in the shear layer in which it resides, but has remarkably little direct influence in the opposite shear layer. The vorticity field during control was taken at $tU_0/D = 150$ of figure 13; for the natural wake, it was taken from the 'quasi-steady' basic state. (The 'quasi-steady' state is the instantaneous flow field which exists immediately prior to the exponential growth of the pure-frequency disturbance leading to vortex shedding; e.g. Hannemann & Oertel (1989). For subcritical Reynolds numbers, the 'quasi-steady' solution is the same as the steady solution of the Navier–Stokes equations. In this analysis, the steady and quasi-steady solutions are quite similar, because the Reynolds number is only slightly above the critical, allowing us to compare the controlled wake with the 'quasi-steady' solution, thus eliminating the need to compute the steady solution separately.)

The control contours always lie outside the locus of maximum vorticity present in the steady wake. To see this, lines of constant vorticity from Dennis & Chang (1970) for a *steady* flow past a circular cylinder at $Re = 70$ are plotted in figure 28, with the dashed line representing the locus of maximum vorticity at each streamwise position. A typical suppression boundary from figure 20 is superimposed. It is clear that the

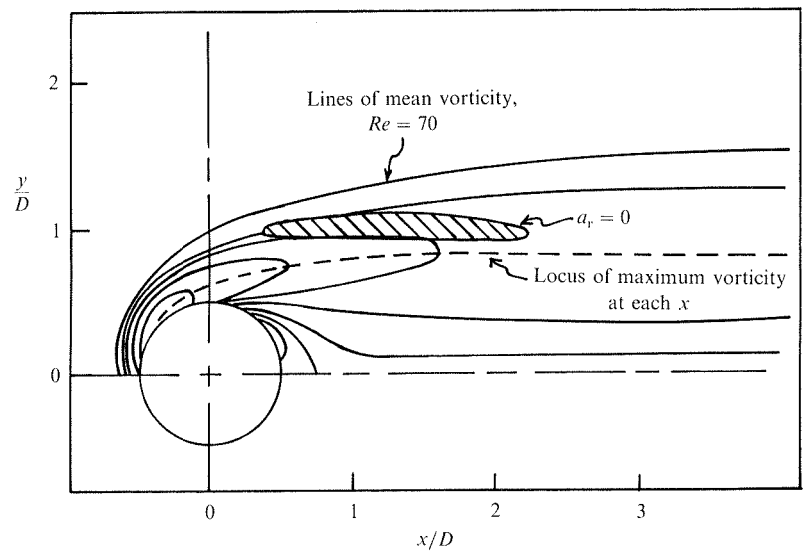

FIGURE 28. Mean vorticity lines plotted with the contour $a_r = 0$ at $Re = 70$. The mean vorticity data are for steady flow at $Re = 70$ from Dennis & Chang (1970).

lower edge of the boundary lies everywhere above the line of maximum vorticity. This conclusion also follows from Dennis & Chang's data at lower Reynolds numbers.

Under these circumstances, a partial cancellation of the vorticity results in the portion of the shear layer closest to the wake centreline. Correspondingly an enhancement of the vorticity must occur farther off-axis; both of these effects can be observed in figure 27(b). To quantify roughly the extent of vorticity diffusion, the circulation in the upper and lower shear layers from figure 27(b) was computed on either side of the wake centreline over a domain from $0.5 < x/D < 4$ and $|y/D| < 1$. The magnitude of the circulation in the upper shear layer (containing the control body) was reduced by over 50% in comparison to that for the lower shear layer. When the domain of integration was extended to larger $|y/D|$ the additional circulation on the high-speed side of the control cylinder began to balance that depleted from the low-speed side. Together, this simply confirms that the upper layer has been effectively diffused.

By the same arguments a control cylinder placement may exist which leads to the enhancement of the circulation of the main shear layer resulting in a destabilization of the wake. But we have not seen that to happen even after a detailed search. We can in general reduce a shear by either decreasing the velocity in the high-speed stream or increasing the velocity in the low-speed stream. It appears that a properly placed control cylinder may satisfy both these criteria by a combination of its velocity defect and its ability to redirect the oncoming flow. Apparently this unique combination is not satisfied in the immediate neighbourhood of the main cylinder, a detail which requires further study.

We may thus conclude that the properly placed control cylinder weakens the shear layer by spreading the velocity gradient over a larger distance; i.e. diffusing vorticity. When the control cylinder is placed farther outside but near to the locus of maximum vorticity, the wake of the control cylinder is most effective in reducing the circulation in that portion of the shear layer which is most critical for vortex

formation. Using the formation-length terminology of Gerrard, a properly placed control cylinder increases the diffusion length, or equivalently, thickens the shear layer. If the circulation is reduced below some threshold level in the formation region, the mutual attraction between the opposing shear layers will be too weak to form the vortex roll-up. Gerrard's model was originally applied only to Reynolds numbers greater than about 90. Although a control cylinder of dimensions $d = \frac{1}{10}D$ was unable to suppress vortex shedding for $Re > 90$, larger control cylinders were capable of vortex suppression up to Reynolds numbers on the order of 150 or more (D. J. Olinger 1986, private communication); the phenomenon at these higher Reynolds numbers is qualitatively similar in all respects to the above discussions. Furthermore the data in figures 11 and 21 indicate no conspicuous behaviour in the neighbourhood of $Re = 90$ which would suggest that the control mechanism has changed significantly. In fact we believe that these results provide some evidence that Gerrard's model is applicable also in the lower Reynolds-number range.

An interesting prediction made by Gerrard was that as the shear layers were weakened, but before the 'vortex street' was eliminated the shedding frequency would be reduced because the weaker shear layers could not as rapidly 'pull' each other across the wake. Consistent with this model, we observe that the weakened shear layers result in a reduced shedding frequency (see figure 11) even when the 'vortex street' is not eliminated.

7.3. *Absolute and convective instabilities*

Although the concepts of absolute and convective instability are strictly valid for describing the space–time evolution of a generic linear disturbance on an infinitely parallel flow, they provide a useful framework for explaining the influence of the control cylinder, and of the vortex shedding mechanism itself. Tentative connections have been indicated by these and other recent experimental studies (see Mathis *et al.* 1984; Strykowski 1986; Provansal *et al.* 1987 and Sreenivasan *et al.* 1987, as well as numerical studies of Koch 1985; Triantafyllou *et al.* 1986; Monkewitz & Nguyen 1987; Hannemann & Oertel 1989 and Triantafyllou & Karniadakis 1990) but the connection still requires careful consideration. It is not entirely clear why the analysis based on these approximations should be relevant to wake flows, but calculations based on these or related ideas yield sensible results (e.g. Koch 1985, and other references cited above). Perhaps the most appropriate way of viewing the problem is through the temporal instability of two-dimensional disturbance eigenfunctions (Jackson 1987; Zabib 1987).

It was found that the natural and controlled wakes are qualitatively similar, and a feature of this study is the use of the control cylinder as an additional parameter for studying the details of the problem. One of the major conclusions of this work is that the suppression of the vortex street corresponds to the global decay of modes that would, under normal circumstances, be temporally amplified. Since none of the control devices worked when placed downstream of x/D around 4 – recall the results of Roshko (1955) on the use of splitter plates which were ineffective in suppressing shedding when placed downstream of approximately $x/D = 3$ – temporally unstable eigenmodes must be very heavily weighted by the near field. Preliminary numerical calculations of Hannemann (1987) provide qualitative indication of the extent to which the eigenmode weighting occurs in the near field of bluff bodies. By introducing a small-amplitude impulse perturbation at several locations behind a flat plate in the quasi-steady state, a region of temporal receptivity was found. At the

Reynolds number of 200, this region extended downstream to approximately 4 trailing-edge thicknesses of the plate and half that distance normal to the flow.

One of us (P.J.S.) expresses thanks to Professor H. Oertel Jr for interest in this work and support for the computational phase of this work, and to Dr W. Koch, Dr K. Hannemann and Professor P. A. Monkewitz for valuable discussions. The other (K.R.S.) acknowledges several useful conversations with Professor M. Morkovin. We are indebted to Professor B.-T. Chu and Mr D. Kyle for a careful reading of the manuscript and to Mr D. Olinger for assisting in gathering the LDV data. The work was supported primarily by a grant from the Air Force Office of Scientific Research.

REFERENCES

Abernathy, F. H. & Kronauer, R. E. 1961 The formation of vortex sheets. *J. Fluid Mech.* **13**, 1–20.

Ahlborn, B. & Lefrancois, M. 1985 Constructive and destructive interference of drag forces in turbulent wakes. *38th meeting of the Fluid Dyn. Div. of the Am. Phys. Soc., Paper* CN3, p. 1727 (abstract only).

Bearman, P. W. 1967 The effect of base bleed on the flow behind a two-dimensional model with a blunt trailing edge. *Aero. Q.* **18**, 207–224.

Bechart, D. W. 1985 Excitation of instability waves. *Z. Flugwiss. W.* **9**, 356–361.

Berger, E. 1964 Bestimmung der hydrodynamischen Grössen einer Karmanschen Wirbelstrasse aus Hitzdrahtmessungen bei Kleinen Reynolds-Zahlen. *Z. Flugwiss. W.* **12**, 41–59.

Berger, E. 1967 Suppression of vortex shedding and turbulence behind oscillating cylinders. *Phys. Fluids Suppl.* **10**, 191–193.

Berger, E. & Wille, R. 1972 Periodic flow phenomena. *Ann. Rev. Fluid Mech.* **4**, 313–340.

Cimbala, J. M., Nagib, H. & Roshko, A. 1988 Large structure in the far wakes of two-dimensional bluff bodies. *J. Fluid Mech.* **190**, 265–298.

Dennis, S. C. R. & Chang, G.-Z. 1970 Numerical solutions for steady flow past a circular cylinder at Reynolds numbers up to 100. *J. Fluid Mech.* **42**, 471–489.

Fage, A. & Johansen, F. C. 1927 On the flow of air behind an inclined flat plate of infinite span. *Proc. R. Lond. Soc. A.* **166**, 170–197.

Fage, A. & Johansen, F. C. 1928 The structure of the vortex street. *Phil. Mag.* **5**, 417–441.

Fornberg, B. 1980 A numerical study of steady viscous flow past a circular cylinder. *J. Fluid Mech.* **98**, 819–855.

Gaster, M. 1969 Vortex shedding from slender cones at low Reynolds numbers. *J. Fluid Mech.* **38**, 565–576.

Gaster, M. 1971 Vortex shedding from circular cylinders at low Reynolds numbers. *J. Fluid Mech.* **46**, 749–756.

Gerich, D. & Eckelmann, H. 1982 Influence of end plates and free ends on the shedding frequency of circular cylinders. *J. Fluid Mech.* **122**, 109–121.

Gerrard, J. H. 1966 The mechanics of the formation region of vortices behind bluff bodies. *J. Fluid Mech.* **25**, 401–413.

Grassberger, P. & Procaccia, I. 1983 Characterization of strange attractors. *Phys. Rev. Lett.* **50**, 346–349.

Hannemann, K. 1987 Numerische Simulation und Stabilitätstheoretische Untersuchung des absolut und konvektiv instabilen Nachlaufs. Ph.D. thesis, Universität Karlsruhe.

Hannemann, K., Gilbert, N., Schwamborn, D. & Gentzsch, W. 1985 A finite-difference Galerkin method for the solution of the Navier-Stokes equations. In *Proc. 6th GAMM Conference on Numerical Methods in Fluid Mechanics, Göttingen, 25–27 September.*

Hannemann, K. & Oertel, H. 1989 Numerical simulation of the absolutely and convectively unstable wake. *J. Fluid Mech.* **199**, 55–88.

HIROTA, I. & MIYAKODA, K. 1965 *J. Met. Soc. Japan* II **43**, 30–36.

HUERRE, P. & MONKEWITZ, P. A. 1985 Absolute and convective instabilities in free shear flows. *J. Fluid Mech.* **159**, 151–161.

JACKSON, C. P. 1987 A finite-element study of the onset of vortex shedding in flow past variously shaped bodies. *J. Fluid Mech.* **182**, 23–45.

KÁRMÁN, TH. VON 1911 Über den Mechanismus des Widerstandes, den ein bewegter Körper in einer Flussigkeit erzeugt. *Nacht. Wiss. Ges. Göttingen. Math. Phys. Klasse*, 509–517.

KÁRMÁN, TH. VON & RUBACH, H. 1912 Über den Mechanismus des Flüssigkeits-und Luftwiderstandes. *Phys. Z.* **13**, 49–59.

KOCH, W. 1985 Local instability characteristics and frequency determination of self-excited wake flows. *J. Sound Vib.* **99**, 53–83.

KOVASZNAY, L. S. G. 1949 Hot-wire investigation of the wake behind cylinders at low Reynolds numbers. *Proc. R. Soc. Lond.* A **198**, 174–190.

MAIR, W. A. & MAULL, D. J. 1971 Bluff bodies and vortex shedding – a report on Euromech 17. *J. Fluid Mech.* **45**, 209–224.

MATHIS, C., PROVANSAL, M. & BOYER, L. 1984 The Bénard–von Kármán instability: an experimental study near the threshold. *J. Phys. Lett.* **45**, L483–491.

MONKEWITZ, P. A. 1988 The absolute and convective nature of instability in two-dimensional wakes at low Reynolds numbers. *Phys. Fluids* **31**, 999–1006.

MONKEWITZ, P. A. & NUYGEN, L. N. 1987 Absolute instability in the near-wake of two-dimensional bluff bodies. *J. Fluids Structures* **1**, 165–184.

MONKEWITZ, P. A. & SOHN, K. D. 1986 Absolute instability in hot jets and their control. *AIAA Paper* 86–1882, presented at the *10th AIAA Aeroacoustics Conference, July 9–11, Seattle.*

NISHIOKA, M. & SATO, H. 1974 Measurements of velocity distributions in the wake of a circular cylinder at low Reynolds numbers. *J. Fluid Mech.* **65**, 97–112.

NISHIOKA, M. & SATO, H. 1978 Mechanism of determination of the shedding frequency of vortices behind a cylinder at low Reynolds numbers. *J. Fluid Mech.* **89**, 49–60.

OLINGER, D. J. & SREENIVASAN, K. R. 1988*a* Nonlinear dynamics of the wake of an oscillating cylinder. *Phys. Rev. Lett.* **60**, 797–800.

OLINGER, D. J. & SREENIVASAN, K. R. 1988*b* Low Reynolds number dynamics in the wake of an oscillating cylinder. In *Proc. ASME Intl Symp. Flow-Induced Vibrations and Noise*, pp. 1–27.

PROVANSAL, M., MATHIS, C. & BOYER, L. 1987 Bénard–von Kármán instability: transient and forced regimes. *J. Fluid Mech.* **182**, 1–22.

ROSHKO, A. 1954 On the development of turbulent wakes from vortex streets. *NACA Rep.* 1191.

ROSHKO, A. 1955 On the wake and drag of bluff bodies. *J. Aero. Sci.* **22**, 124–132.

SHAIR, F. H., GROVE, A. S., PETERSEN, E. E. & ACRIVOS, A. 1963 The effect of confining walls on the stability of the steady wake behind a circular cylinder. *J. Fluid Mech.* **17**, 547–550.

SREENIVASAN, K. R. 1985 Transition and turbulence in fluid flows, and low-dimensional chaos. In *Frontiers of Fluid Mechanics* (ed. S. H. Davis & J. L. Lumley), pp. 41–67. Springer.

SREENIVASAN, K. R. 1986 Chaos in open flow systems. In *Dimensions and Entropies in Chaotic Systems* (ed. G. Mayer-Kress), pp. 222–230. Springer.

SREENIVASAN, K. R., RAGHU, S. & KYLE, D. 1989 Absolute instability in variable density jets. *Exps. Fluids* **7**, 309–317.

SREENIVASAN, K. R., STRYKOWSKI, P. J. & OLINGER, D. J. 1986 Hopf bifurcation, Landau equation, and vortex shedding behind circular cylinders. In *Proc. Forum on Unsteady Flow Separation* (ed. K. N. Ghia), pp. 1–13. ASME.

STANSBY, P. K. 1974 The effects of end plates on the base pressure coefficient of a circular cylinder. *Aero. J.* **78**, 36–37.

STEPHENS, A. B., BELL, J. B., SOLOMON, J. M. & HACKERMAN, L. B. 1984 A finite-difference Galerkin formulation for the incompressible Navier–Stokes equations, *J. Comput. Phys.* **53**, 152–172.

STROUHAL, V. 1878 Über eine besondere Art der Tonerregung. *Ann. Phys. Chemie* (*New series*) **5**, 216–251.

STRYKOWSKI, P. J. 1986 The control of absolutely and convectively unstable shear flows. Ph.D. thesis, Engineering and Applied Science, Yale University.

STRYKOWSKI, P. J. & SREENIVASAN, K. R. 1985*a* The control of transitional flows. *AIAA Shear Flow Control Conf. Boulder, Colorado, Paper* 85–0559.

STRYKOWSKI, P. J. & SREENIVASAN, K. R. 1985*b* The control of vortex shedding behind circular cylinders at low Reynolds numbers. *Proc. 5th Symp. on Turb. Shear Flows, Cornell Univ., Ithaca.*

THOMAN, D. C. & SZEWCZYK, A. A. 1969 Time-dependent viscous flow over a circular cylinder. *Phys. Fluids Suppl.* **12**, II 76–86.

TRIANTAFYLLOU, G. S. & KARNIADAKIS, G. EM. 1990 Computational reducability of unsteady viscous flow. *Phys. Rev. Lett.* (submitted).

TRIANTAFYLLOU, G. S., TRIANTAFYLLOU, M. S. & CHRYSSOSTOMIDIS, C. 1986 On the formation of vortex streets behind stationary cylinders. *J. Fluid Mech.* **170**, 461–477.

TRITTON, D. J. 1959 Experiments on the flow past a circular cylinder at low Reynolds numbers. *J. Fluid Mech.* **6**, 547–567.

WEHRMANN, O. H. 1967 Influence of vibrations on the flow field behind a cylinder. *Phys. Fluids Suppl.* **10**, 187–190.

ZABIB, A. 1987 Stability of viscous flow past a circular cylinder. *J. Engng Maths* **21**, 155–165.